

FZD-507

Wissenschaftlich-Technische Berichte  
FZD-507 2009 · ISSN 1437-322X

# Advanced Materials Research

BIENNIAL SCIENTIFIC REPORT 2007-2008 | Volume 1



Forschungszentrum  
Dresden Rossendorf

**Cover picture:** PhD student Jing Zhou at the atomic force microscope of the Ion-Beam Center at the Forschungszentrum Dresden-Rossendorf.  
Photo: Rainer Weisflog

## IMPRINT

### FZD Biennial Scientific Report 2007-2008 | Volume 1

Volume 1                   Advanced Materials Research  
Volume 2                   Cancer Research  
Volume 3                   Nuclear Safety Research

**Published by**                   Forschungszentrum Dresden-Rossendorf  
**Concept and editorial work** Dr. Christine Bohnet & Anja Bartho, FZD  
**Design and layout**           WA Preußel, Coswig  
**Photos**                         FZD employees  
**Available from**               Forschungszentrum Dresden-Rossendorf  
Public Relations  
Bautzner Landstr. 400  
01328 Dresden / Germany  
Phone: +49 351 260 2450  
Email: [contact@fzd.de](mailto:contact@fzd.de)  
<http://www.fzd.de>

### ISSN 1437-322X

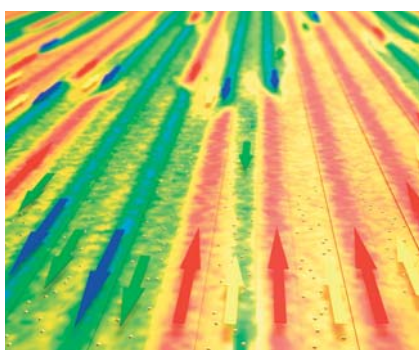
Wissenschaftlich-Technische Berichte  
FZD-507, March 2009

Copying is welcomed, provided the source is quoted.

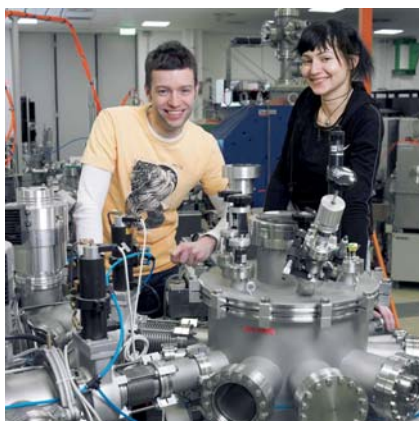
In addition to the Biennial Scientific Reports, the Annual Online Report of the FZD, with research and other highlights of the past year, is available under: [www.fzd.de/online-report](http://www.fzd.de/online-report)

# Content

FOCUS



FACILITIES



RESEARCH



FACTS & FIGURES



<b>PREFACE</b> .....	2
<b>FOCUS</b> .....	4
HADES solves the DLS puzzle .....	6
<b>FACILITIES FOR EUROPE</b>	
The Radiation Source ELBE .....	8
The Free-Electron Lasers at the FZD .....	10
The Dresden High Magnetic Field Laboratory (HLD) .....	12
The Ion-Beam Center .....	14
Materials research with synchrotron radiation at ROBL .....	17
<b>RESEARCH</b>	
Magnetic control of temperature fluctuations in crystal growth processes .....	20
An exotic high-field state of superconductivity .....	22
Coupling of the free-electron laser facility with pulsed magnetic fields: first results .....	24
Superconductivity in doped semiconductors .....	26
New antennas for bridging the terahertz gap .....	28
Magnetic zinc oxide .....	30
Self-organized surface nanopatterns induced by low-energy ion erosion .....	32
Commissioning of the superconducting radiofrequency photoelectron injector at ELBE .....	34
<b>FACTS &amp; FIGURES</b> .....	37

# Preface

---



Roland Sauerbrey  
*Scientific Director*

The mission of the Forschungszentrum Dresden-Rossendorf (FZD) is excellence in long-term research in socially important issues like energy, health, and advanced material technologies. In strategic collaborations with partners from research and industry the FZD contributes to solve major challenges of modern society. Scientific work at the research center focuses on three questions:

- ◆ How does matter behave in strong fields and at small dimensions?
- ◆ How can cancerous tumors be identified in the early stages and treated effectively?
- ◆ How can the public and the environment be protected from technical risks?

Corresponding to these questions, the Forschungszentrum Dresden-Rossendorf pursues the three program topics "Advanced Materials Research", "Cancer Research", and "Nuclear Safety Research". This Biennial Scientific Report highlights the scientific achievements of the "Advanced Materials Research" program, covering the years 2007 and 2008. The first part introduces the overall focus of the program as well as the large-scale facilities that are used for research, and the second part consists of eight articles highlighting research projects that were conducted by scientists of the following institutes:

- ◆ Dresden High-Magnetic Field Laboratory
- ◆ Ion-Beam Physics and Materials Research
- ◆ Safety Research
- ◆ Radiation Physics

In 2007, the FZD was evaluated by the German Council of Science and Humanities (Wissenschaftsrat). In its final evaluation report, published in July 2008, the Council unanimously recommended that the FZD – a Leibniz institution – should become a member of the Helmholtz Association. The report emphasizes: "Since the last evaluation by the German Council of Science and Humanities, the FZD has continuously worked on long-term and highly complex research topics, thus expanding its scientific profile towards a major research center. This top-level research on a strategic and long-term basis in politically and socially important issues suggests an increased financial commitment of the Federal Republic of Germany."

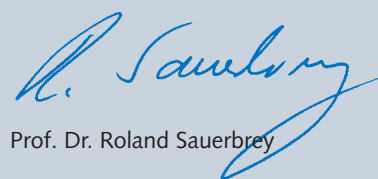
To highlight a few noteworthy events in 2007 and 2008, one must mention the magneto-hydrodynamic (MHD) project of the FZD, which forms a major part of the Collaborative Research Center (SFB) 609 "Electromagnetic flow control in metallurgy, crystal growth, and electrochemistry". The German Science Foundation (DFG) decided in autumn 2008 to prolong the funding for another four years. Moreover, Dr. Frank Stefani, member of the MHD group, and Prof. Günther Rüdiger (Astrophysikalisches Institut Potsdam, AIP) earned the highly prestigious "Society needs Science 2008" award of the "Stifterverband für die deutsche Wissenschaft" for the first experimental demonstration of the magneto-rotational instability. The PROMISE experiment (Potsdam Rossendorf Magnetic InStability Experiment) was conducted in close collaboration between FZD and AIP.

Networks and funding on a European level play an ever increasing role for our research and large-scale facilities. The free-electron lasers at ELBE have been funded as user facilities for several years now, and the same is true for the Ion-Beam Center of the Institute of Ion-Beam Physics and Materials Research. This Institute has been very successful in acquiring a project within the 7<sup>th</sup> framework program of the EU named SPIRIT (Support of Public and Industrial Research using Ion Beam Technology). Under the Institute's coordination, SPIRIT offers transnational access to European users from 2009 to 2013. Last but not least, the Dresden High-Magnetic Field Laboratory, as member of a European network of the four leading high-magnetic field facilities, provides a unique environment for the investigation of solid-state materials in very high magnetic fields to users from all over the world. For now, the Institute holds the European pulsed field record of 87.2 Tesla, which is a mere 2 Tesla short of the world record.

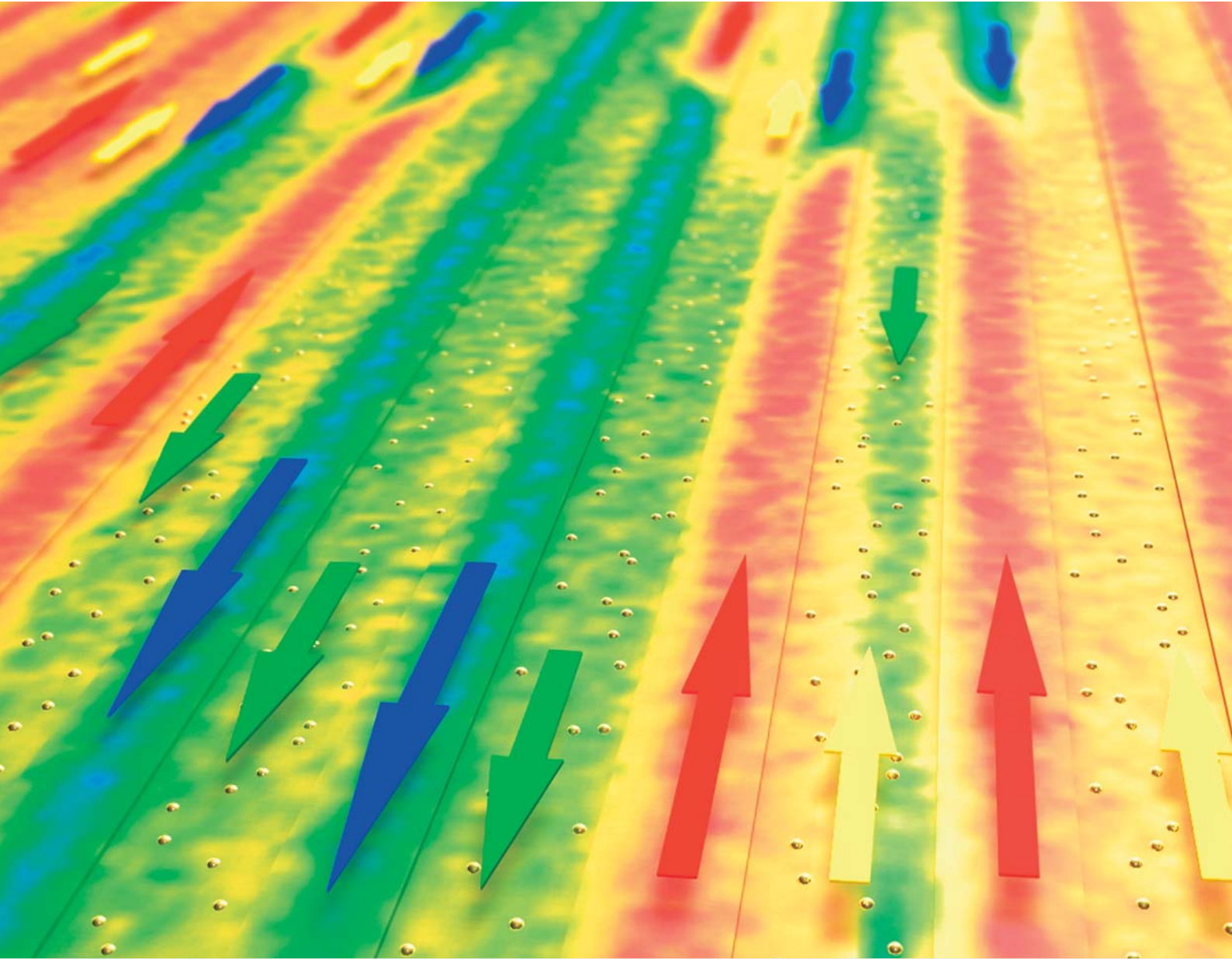
To further strengthen the international visibility of the FZD in the scientific community, the FZD served as the local organizer of the IEEE Meetings "Medical Imaging Conference (MIC)" and "Nuclear Science Symposium (NSS)". The 2008 IEEE-NSS-MIC Conference took place in Dresden from October 19 to 25, and scientists of the Advanced Materials Research program were actively engaged in it. Several aspects of the Radiation Source ELBE, for example the newly commissioned superconducting radiofrequency gun, were presented by scientists of the Institute of Radiation Physics, and more than 100 conference attendees took the opportunity to visit the ELBE facility at the FZD. All in all, the Dresden IEEE Conference attracted more than 2,700 participants, thus being the largest IEEE-NSS-MIC Conference ever. We are very grateful to the German Science Foundation (DFG) and the Saxon State Ministry of Higher Education, Research and the Arts (SMWK) for their essential contributions of funding for the Conference.

The success of a research institution strongly depends on the motivation and dedication of talented young scientists. The FZD has put a lot of effort into attracting junior scientists from Germany and abroad. Our six institutes strive for excellent working conditions and support of their staff, the FZD as a whole offers Ph.D. seminars to about 120 doctoral students, a tenure track program for outstanding postdoctoral staff, special workshops for young scientists such as communication to the media, presentation in English, training for young science managers, etc. The FZD supports high-level training as well for its technical staff and its almost 60 trainees. In 2008, the FZD received the "Audit Beruf und Familie" (Career and Family Certificate) from the Hertie Foundation, underlining the particular importance attached to the healthy balance of family and career at the FZD.

Finally, this preface gives me the opportunity to thank our funding institutions, the Saxon State Ministry of Higher Education, Research and the Arts (SMWK) and the Federal Ministry of Education and Research (BMBF), for their continued support, our national and international scientific cooperation partners for many successful joint research endeavors, and the entire staff of the FZD for their dedicated work.



Prof. Dr. Roland Sauerbrey



# Advanced Materials Research program

at the Forschungszentrum Dresden-Rossendorf

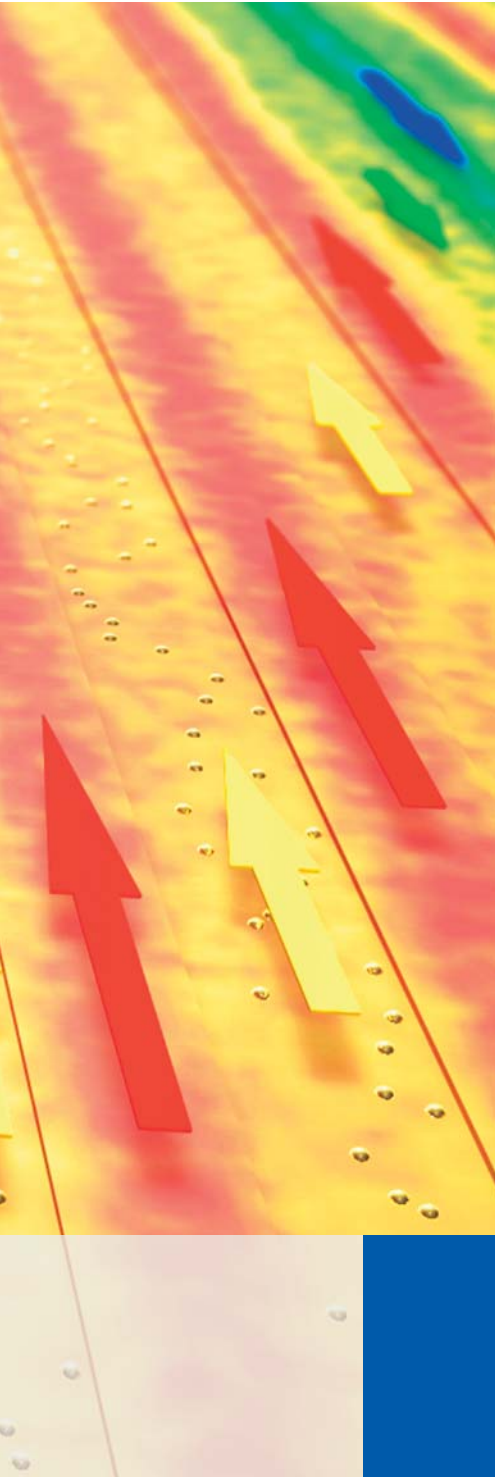
Wolfhard Möller, Manfred Helm,  
Joachim Wosnitza, Thomas E. Cowan

Advanced Materials Research addresses the response of matter to extreme irradiation conditions, and to electric and magnetic fields. Fast ions are employed for the development of new materials with a prominent focus on nanosystems. Novel structural and functional properties are investigated using techniques with ultrahigh spatial and temporal resolution. Research with high magnetic fields is concerned with the electronic properties of condensed matter using strong pulsed magnetic fields. Magneto-hydrodynamics

research aims at customizing the flow of electrically conducting fluids in metallurgy and crystal growth by applying magnetic fields, in order to optimize the manufacturing processes and to improve the quality of castings and crystals. Subatomic physics studies, including rare hadronic processes in matter and nuclear processes, are relevant to materials in nuclear technology, as well as to the development of new radiation sources and instrumentation for Advanced Materials Research.

For these topics, the FZD offers four large-scale experimental infrastructures. The Ion-Beam Center (IBC) houses ion-beam and

plasma devices that deliver ions at energies between approximately 10 eV and 50 MeV for surface modification and analysis, as well as for ion-assisted thin-film deposition. Ion beams are used to create high-performance materials with specific and often nanostructure-based functions for electronic, optical, and magnetic applications. In addition to the in-house research activities, the Ion-Beam Center serves as a national and international user facility for research and industry, and is funded within the European Commission's Transnational Access program.



The Rossendorf Beamline at the European Synchrotron Radiation Facility (ESRF), located in Grenoble, contributes to materials research at the FZD, offering X-ray diffraction and reflection, particularly in several real-time in-situ devices for thermal treatment and thin-film deposition.

The Dresden High Magnetic Field Laboratory (HLD) has set an ambitious goal to provide 100 Tesla in millisecond pulses for materials research, in order to study the electronic properties of advanced materials such as high-temperature superconductors, magnets, or semiconductors, also in combination with the ELBE free-electron lasers. The HLD operates as an international user research facility, and is funded by the European Commission to provide transnational access.

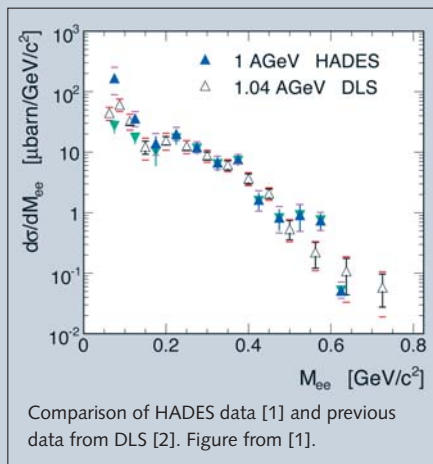
The Radiation Source ELBE provides numerous particle and photon beams. Its electron beam is applied both directly and through the production of high-energy photons, neutrons, and positrons. Two attached free-electron lasers deliver high-intensity coherent infrared light used primarily for the study of semiconductor materials. They are also funded by the European Commission and provide transnational access to external users. The new high-intensity laser "Draco" in the ELBE laboratory has been commissioned, which will enable, for example, laser acceleration of ions. These will be used for multi-disciplinary studies of non-linear particle-matter interaction.

These large-scale facilities support the goal of increasingly interlinking the activities of the three FZD programs. Biological templating of metallic nanostructures, physico-chemical characterization of radionuclide complexes, measurement of transmutation cross-sections, and tomographic characterization of pulsed magnet coils are additional examples of internal interdisciplinary cooperation with the Cancer Research and the Nuclear Safety Research program. Special emphasis is also given to close collaborations with other research institutions, especially with the Technische Universität Dresden. For example, the magneto-hydrodynamic (MHD) project of the FZD forms a major part of the Collaborative Research Center (SFB) 609 "Electromagnetic flow control in metallurgy, crystal growth, and electrochemistry", which is funded by the German Science Foundation (DFG).

# HADES solves the DLS puzzle

Roland Kotte, Lothar Naumann,  
Jörn Wüstenfeld, Burkhard Kämpfer

In large accelerators like the heavy-ion synchrotron SIS18, or FAIR (Facility for Antiproton and Ion Research) currently under construction at the GSI in Darmstadt, particle collisions result in the production of a variety of exotic or rare particles, for example the so-called vector mesons. These can be detected by their decay into “dileptons,” which are correlated pairs of either an electron and positron ( $e^-/e^+$ ), or a positive and negative muon ( $\mu^-/\mu^+$ ). Many theoretical models, ranging from hadronic interactions to evaluations of the theory of strong



interaction, predict a change of the properties of vector mesons when they are embedded in the strongly interacting medium during the course of the heavy-ion collisions. The dileptons, however, leave the interaction zone undisturbed, and therefore provide a direct probe of the spectral distribution of the vector mesons. Such direct probes are believed to monitor the various collision stages in nuclear reactions, and they also carry implicit information on the origin of the masses of the strongly interacting particles involved.

One important physics result of the first round of experiments with the second generation detector installation HADES

(High Acceptance Di-Electron Spectrometer) at the heavy-ion synchrotron SIS18 at GSI was the solution [1] of the DLS puzzle. The Dilepton Spectrometer (DLS) collaboration had published, after some pioneering experiments, a data analysis which corrects previous results by a factor of 8 [2]. However, the dilepton spectrum could not be explained in a convincing manner by many attempted model calculations. This puzzle caused doubts in the validity of the DLS data, but has now been clarified by the agreement with HADES data (see Fig.).

The key issue in a convincing interpretation [3] of the data [1, 2] involved a proper treatment of bremsstrahlung contributions according to [4]. Having understood the overall pattern of the dilepton radiation in the collision of light nuclei at beam energies in the 1-2 AGeV range, one can now search for interesting in-medium modifications of the vector mesons, such as predicted in [5, 6] for example. In doing so, the performance of HADES has been improved, e.g. by equipping some of the time-of-flight instruments with resistive plate chambers, which allow for a much better timing resulting in better particle identification.

The timing properties and the radiation hardness of resistive plate chambers are presently tested at the Radiation Source ELBE of the FZD, making use of the excellent time structure of its bunches [7]. Moreover, to ensure the long-term operation of HADES, particularly into the future also at FAIR, new multi-wire drift chambers for improved tracking are being constructed in the FZD advanced detector workshop. The technological requirements are challenging, but our experience with the previous construction and production of larger multi-wire drift chambers for the third HADES tracking plane ensures to meet the precision and stability criteria. The involvement of our hadron physics group in the instrumentation of HADES

assures our participation within the large international HADES collaboration addressing important questions of heavy-ion and hadron physics. The experiments will be continued by a new, even more complex detector system with the Compressed Matter Collaboration (CBM). CBM includes about 400 participants and will work with higher beam energies available at FAIR, in order to achieve a stronger compression of the nuclear matter and thus providing a better handle for understanding the origin of masses of strongly interacting particles representing the majority core of the visible matter in the universe.

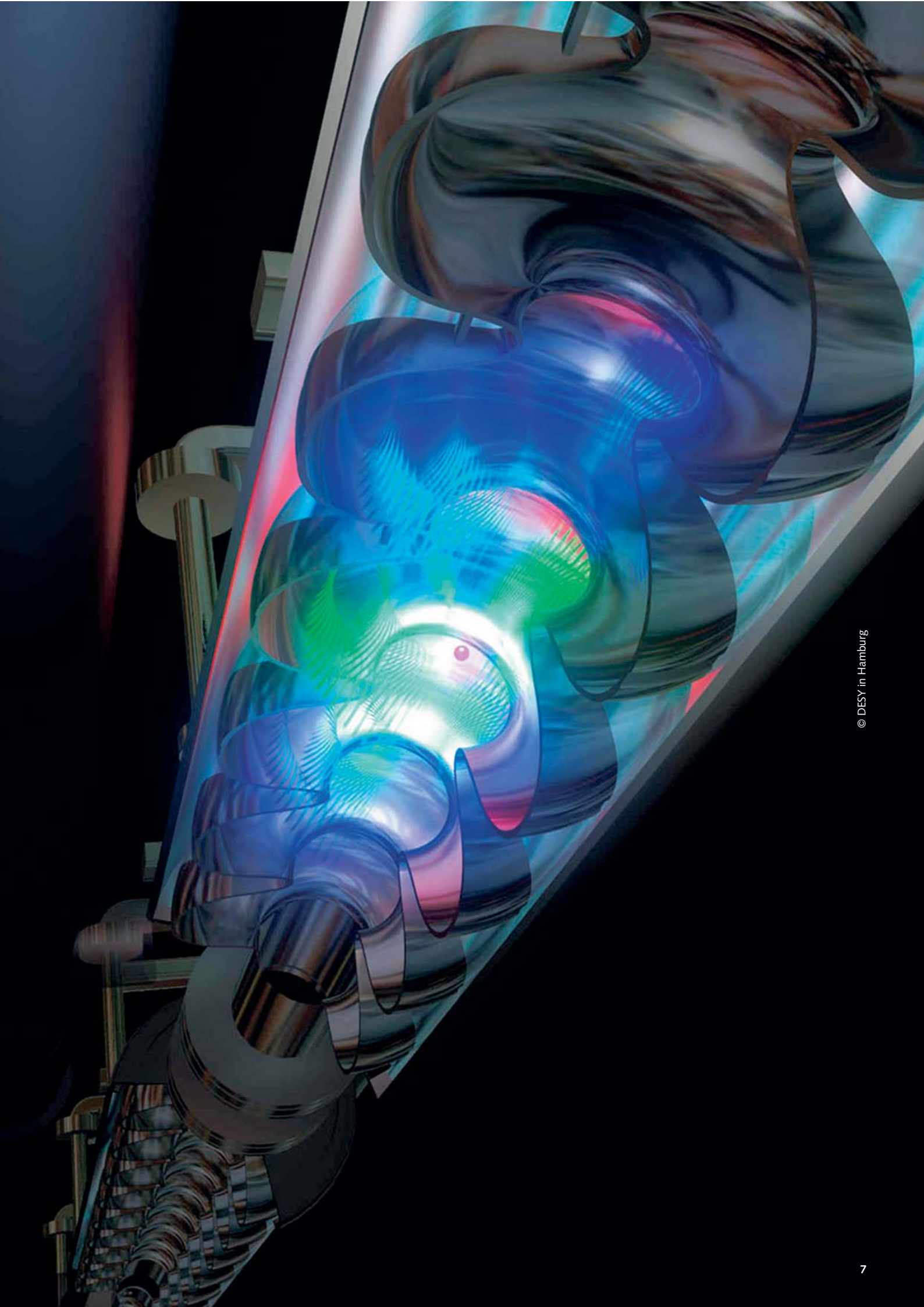
## References

- [1] *Study of dielectron production in C+C collisions at 1 AGeV*, HADES Collaboration (G. Agakishiev et al.), *Physics Letters B* 663, 43 (2008); *Study of dielectron production in C+C collisions at 1 AGeV*, HADES Collaboration (Y. Pachmayer et al.), *Journal of Physics G* 35, 104159 (2008)
- [2] *Dielectron cross-section measurements in nucleus-nucleus reactions at 1 AGeV*, DLS Collaboration (R.J. Porter et al.), *Physical Review Letters* 79, 1229 (1997)
- [3] *Dilepton production and off-shell transport dynamics at SIS energies*, E.L. Bratkovskaya, W. Cassing, *Nuclear Physics A* 807, 214 (2008)
- [4] *Di-electron bremsstrahlung in intermediate-energy pn and Dp collisions*, L.P. Kaptari, B. Kämpfer, *Nuclear Physics A* 764, 338 (2006)
- [5] *Evidence for in-medium changes of four-quark condensates*, R. Thomas, S. Zschocke, B. Kämpfer, *Physical Review Letters* 95, 232301 (2005)
- [6] *In-medium modification and decay asymmetry of omega mesons in cold nuclear matter*, A.I. Titov, B. Kämpfer, *Physical Review C* 76, 065211 (2007)
- [7] *Testing timing RPC detectors at the Rossendorf electron linac ELBE*, R. Kotte et al., *Nuclear Instruments and Methods A* 564, 155 (2006)

## Collaborations

- HADES Collaboration
- CBM Collaboration





# The Radiation Source ELBE



Peter Michel, Thomas E. Cowan

By studying the interaction of various forms of radiation with matter in atomic and subatomic dimensions as well as with tissues, cells, and their components, we can gain a wide range of new insights into their structures and functionalities. Experiments conducted at the Radiation Source ELBE (Electron Linear accelerator with high Brilliance and low Emittance) make an essential contribution to the FZD's research programs. These include experiments using the primary electron beam of the ELBE accelerator, as well as its many secondary particle and radiation beams (infrared photons, X-rays, gamma-rays, neutrons, and positrons). The linear

acceleration consists of two superconducting sections, each cooled to liquid helium temperature, and powered by a continuous-wave radiofrequency (RF) source of 40 kW at 1.3 GHz. Electrons are injected from either a thermally- or laser-excited source, bunched at the RF frequency, and accelerated in a quasi-continuous beam of from 5 MeV up to 40 MeV, with a high average current of up to 1 mA. The electron beam is of especially high quality, characterized by a low transverse emittance (less than 10 mm mrad) and short pulses (typically 2 ps bunch length) with low energy spread and flexible temporal structure. The unusual properties of low emittance, high average current, and high bunch repetition rate

operation make ELBE an ideal source for producing a variety of secondary radiation beams for the various experiments. These include:

(i) Two Free-Electron Lasers (FELs), having undulators of 27 mm and 100 mm period length, which deliver coherent radiation in the mid- and far-infrared. The wavelength of the U27-FEL ranges from 3.5 to 22  $\mu\text{m}$  while the U100-FEL covers 20 to 250  $\mu\text{m}$ . Depending on the IR wavelength, several watts of optical power can typically be extracted. The infrared light beams are transported to several optical laboratories, where a broad range of different experiments are conducted. The primary fields of research include time resolved semiconductor spectroscopy (pump-probe studies) and near-field microscopy. An additional transfer system directs the FEL light to the neighboring Dresden High Magnetic Field Laboratory (HLD), for spectroscopy in strong magnetic fields.

(ii) The high primary electron-beam current allows generation of intense secondary beams of neutrons, either in reactions with a rotating tungsten disc or a liquid-lead target. The emerging neutron pulses carry the time structure of the primary electron beam. This enables time-of-flight experiments to measure neutron-induced nuclear reactions as a function of the incident neutron energy. An extensive program of fast neutron reactions (scattering, absorption, and neutron-induced fission) is now underway to provide important data for nuclear reactor materials, for transmutation of nuclear waste, and for certain steps in the creation of the chemical elements in the early universe and in stars.

(iii) Irradiating a thin foil with the primary electron beam generates hard X-rays with energies up to 20 MeV. By exposing

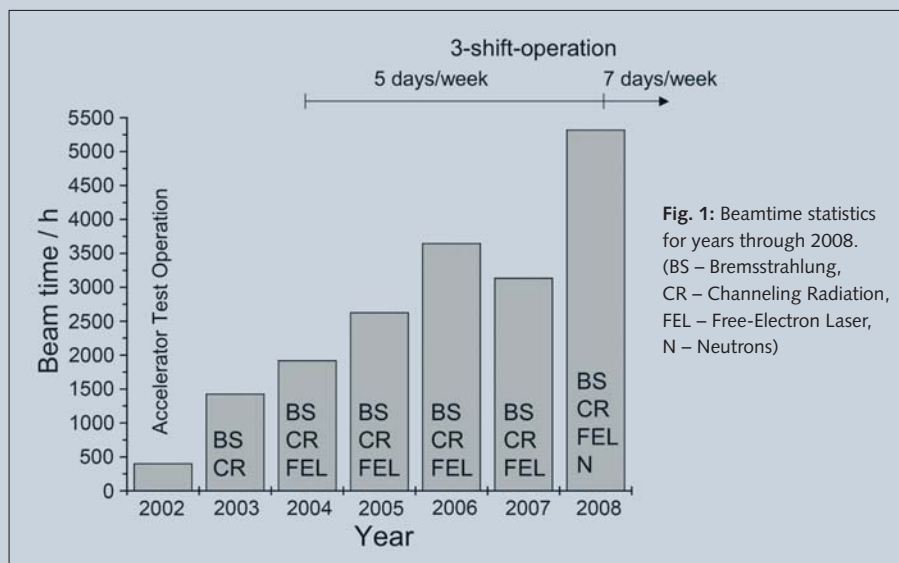


Fig. 1: Beamtime statistics for years through 2008. (BS – Bremsstrahlung, CR – Channeling Radiation, FEL – Free-Electron Laser, N – Neutrons)

selected isotopes to these X-rays, their excitation and transformation into other isotopes through various reactions are studied. This extends the range of nuclear reactions that are investigated with the neutron beam (item ii), and contributes to the research towards nuclear waste transmutation and nucleosynthesis of the elements in stellar explosions. The MeV X-rays are also used to study medical imaging technologies based on positron emission tomography (PET), in which the annihilation gamma-rays from positrons (anti-matter electrons) produced by the beam in tissue are detected. Measurement of the 0.2 to few nanosecond lifetimes of the positrons, with the aid of their sharp time structure, is also used to detect point defects and vacancies with high sensitivity in metals, glasses, and other materials.

(iv) Intense low energy beams of positrons are also produced by the irradiation of stacks of tungsten foils. These are extracted, accelerated, and further bunched, to provide a secondary beam of tunable monoenergetic positron pulses for a variety of new materials science investigations.

(v) The propagation of the well-collimated primary electron beam through crystals, such as diamonds, generates channeling radiation, i.e. X-rays in the 10 to 100 keV range. These X-rays have been used to investigate cell damage for radiobiological studies, as a function of the X-ray energy and dose rate.

(vi) The excellent time structure, and high repetition rate of the primary ELBE beam, enables the development and testing of state-of-the-art detectors with excellent time resolution (below 100 ps) and good stability in a high rate environment – between 10,000 and 50,000 charged particles impinging on the detector per  $\text{cm}^2$  per second. These detectors fulfill the challenging requirements of new experiments at the future Facility for Antiproton and Ion Research (FAIR), as well as for new applications in neutron, particle, and medical physics.

The quality of the primary electron beam from ELBE depends strongly on the electron source (i.e. the electron gun). ELBE was first put into operation with a thermionic gun. Several years of research and development have culminated in the installation and preliminary operation of a new superconducting radio frequency (SRF) gun. First tests have been successful, and further development will enable higher-charge electron bunches, at somewhat reduced frequency, promising to improve the quality and extend the range of experiments possible with the neutron, positron, and X-ray secondary beams.

Fig. 1 displays the beamtime statistics for each year of ELBE operation, and reflects the steady improvement in machine operation and beam quality. The jump in 2008 demonstrates the introduction

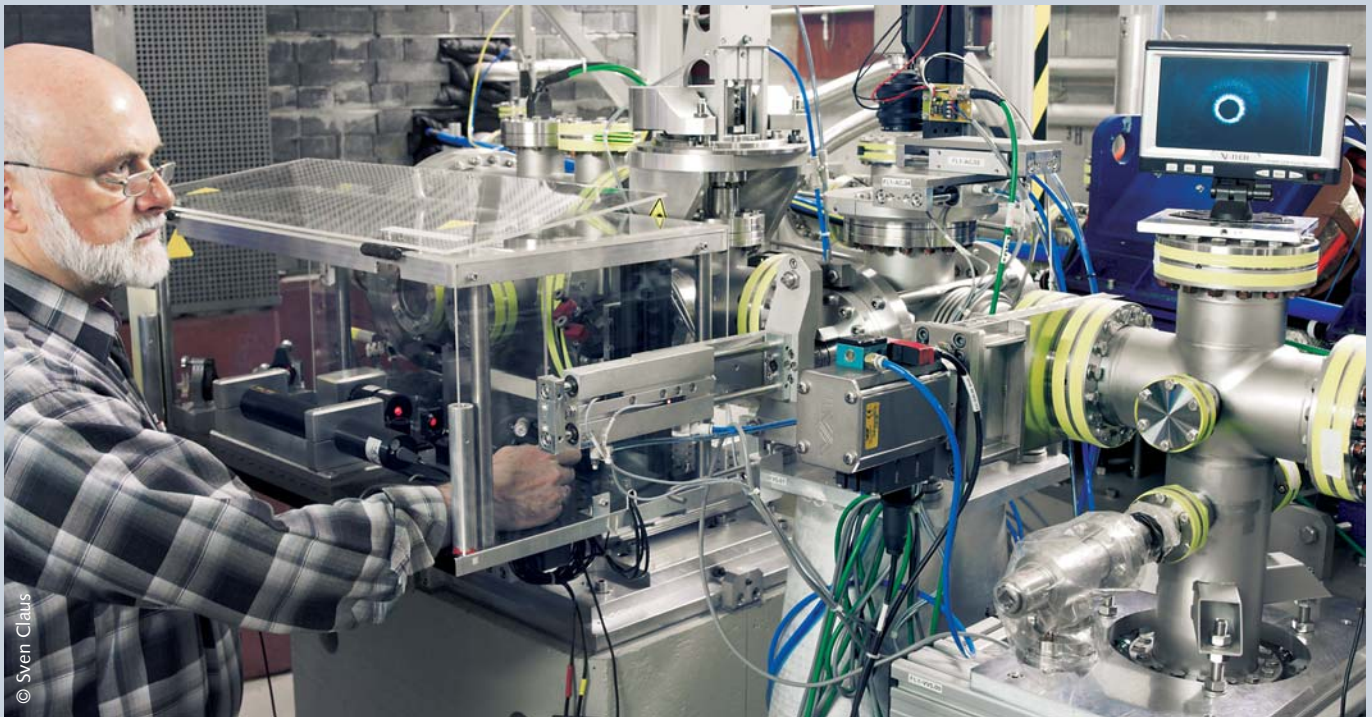
of 7 day per week operation in October, as well as the overall improvement in the operational availability of ELBE in 2008 of 90 %. The useable beam delivered to experiments grew from 58 % in 2007 to 88 % in 2008, with allocations of 33 % to FEL operation, 15 % for neutrons, 12.5 % for MeV X-rays, 9.5 % for channeling radiation, and 1 % for positron source development. In addition to the routine beam operation in scientific experiments, approximately 28 % of the beamtime was used for machine studies using the accelerator and secondary radiation targets. Through May 2008, 22 papers were published based on ELBE experiments.

At present, the ELBE user community is primarily composed of internal users at the FZD; external users account for about 20 % of usage. Internal users come from almost all institutes of the FZD. Of these, about 65 % are from the Institute of Radiation Physics. In addition to German groups from Technische Universität Dresden, Forschungszentrum Karlsruhe, Technische Universität München, and Berliner Elektronenspeicherring-Gesellschaft für Synchrotronstrahlung (BESSY), several external users came from other European Union and nearby countries (University of Linz, Sheffield University, Vilnius University, et cetera) and were supported within the framework of the European Union-funded “Integrated Activity on Synchrotron and Free-Electron Laser Science” (IA-SFS) program.

## References

- [1] *RF status of superconducting module development suitable for cw operation: ELBE cryostats*, J. Teichert, H. Büttig, P. Michel, U. Lehnert, C. Schneider, K. Möller, A. Büchner, F. Gabriel, J. Stephan, A. Winter, *Nuclear Instruments and Methods A* 557, 239 – 242 (2006)
- [2] *A high-brightness SRF photo injector for FEL light sources*, A. Arnold, H. Büttig, D. Janssen, T. Kamps, G. Klemz, W.D. Lehmann, U. Lehnert, D. Lipka, F. Marhauser, P. Michel, K. Möller, P. Murcek, Ch. Schneider, R. Schurig, F. Staufenberg, J. Stephan, J. Teichert, V. Volkov, I. Will, R. Xiang, *Nuclear Instruments and Methods A* 593, 57 – 62 (2008)

# The Free-Electron Lasers at the FZD



Manfred Helm

Free-electron lasers (FEL) differ from conventional lasers in that they do not have an active medium with population inversion between specific energy levels, but rather it is only free electrons, wiggling through a periodic magnetic field arrangement at relativistic speed, which provide stimulated emission and optical gain. Because the emitted wavelength depends only on the energy of the electrons and the magnetic field strength, in principle arbitrary lasing wavelengths may be achieved. Thus, FELs are used primarily in spectral ranges which cannot be attained, at reasonable power levels, by conventional lasers. This is true for the long-wavelength infrared and terahertz (THz) range, and also for the short-wavelength ultraviolet range. In order

to reach the ultraviolet range, very high electron energies in the GeV range are necessary, requiring hundreds of meter long electron accelerators, and only recently such lasers have been constructed.

For the infrared and THz range, however, modest electron energies of some tens of MeV are sufficient, and it is this type which is available at the FZD. This spectral range is well suited to excite and study so-called low-energy excitations in solid and soft matter, such as vibrations, or collective electronic excitations.

The free-electron lasers at the FZD are driven by the superconducting electron linear accelerator ELBE (see article on page 8), which provides short (picosecond) electron bunches with energies up to 40 MeV at a 13 MHz repetition rate.

These electron bunches are fed into an optical cavity whose (doubled) length exactly matches the time interval between subsequent electron pulses (i.e. cavity round trip time =  $1/13 \text{ MHz} = 77 \text{ ns}$ ). The periodic magnetic field arrangement, called an undulator, is placed in the center of the cavity, and it is there that the electrons generate radiation when their path is bent by the magnetic field.

There are two undulators at the FZD – one with a magnetic field period of 27 mm (called U27) for the mid-infrared spectral range (wavelengths 3.5 – 22  $\mu\text{m}$ ) and one having a period of 100 mm (called U100) for the far-infrared or THz range (wavelengths 20 – 250  $\mu\text{m}$ ). These two FELs were given the name FELBE, which stands for FEL at ELBE.

The key feature which distinguishes FELBE from other FEL user facilities is the possibility of "quasi cw" operation (i.e. a continuous train of pulses, also called micropulses), made available by the superconducting accelerator cavities. The FEL thus provides picosecond optical pulses at a repetition rate of 13 MHz. In this mode, the average power can reach up to 30 W (depending on the wavelength), corresponding to more than  $1 \mu\text{J}$  pulse energy.

FELBE is operated as a user facility, i.e. scientists from other institutions are invited to submit short research proposals and

apply for beamtime. Users from the EU and associated countries are funded through an EU grant ("transnational access"). A significant amount of FEL beamtime is also used by FZD scientists for internal research projects, after selection through the formal proposal review procedure.

In order to pinpoint interesting scientific experiments using the FEL, the unique features of FELBE have to be considered: (1) Short pulses (1 – 10 ps, depending on the wavelength), allowing for high time resolution in the study of fast dynamical processes in matter;

(2) High peak power (up to 1 MW) for studying nonlinear processes in matter; (3) High average power (tens of Watts) for applications with tiny interaction cross sections.

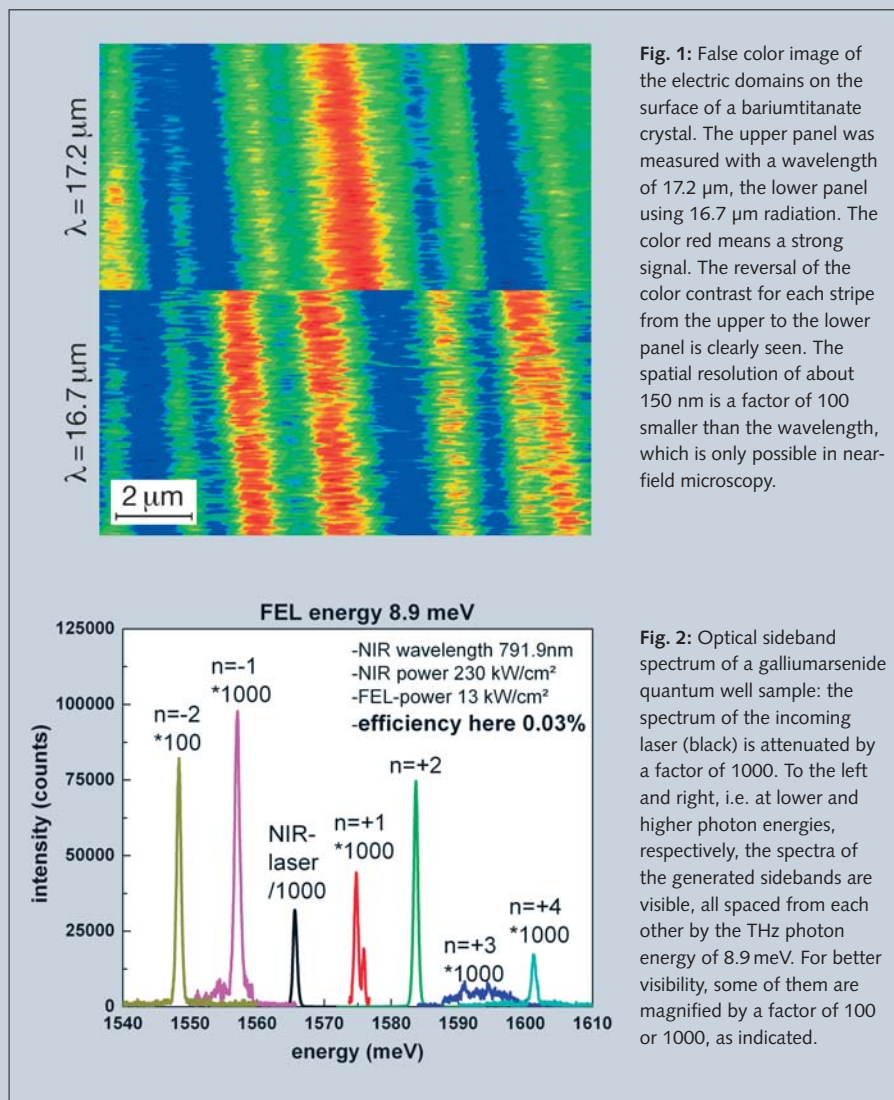
An example for the latter is near-field microscopy and spectroscopy, where the optical signal scattered from a metallic tip in the close vicinity of a sample is measured. Fig. 1 shows a false color image of ferroelectric domains in a bariumtitanate ( $\text{BaTiO}_3$ ) crystal. The lower part is measured using a wavelength of  $16.7 \mu\text{m}$ , the upper part at  $17.2 \mu\text{m}$ . The domains are clearly seen as stripes, and in addition the colors change when the wavelength is altered. This is a contrast reversal, which results from tuning the FEL across a vibrational resonance of the crystal [1].

An example of a nonlinear optical process is the generation of THz sidebands of optical radiation. In a semiconductor sample of galliumarsenide (GaAs) quantum wells, the incoming near-infrared light (wavelength 792 nm) is mixed with the high-power THz radiation of the FEL (wavelength  $140 \mu\text{m}$ , corresponding to a photon energy of 8.9 meV). This results in the generation of near-infrared light with photon energies that differ from the original one by integer multiples of the THz photon energy, as shown in Fig. 2. Such a process finds application in optical signal processing and communication technology, but also yields insights into the microscopic physics of the nonlinear material.

At the FZD, experiments using FEL radiation in a pulsed magnetic field are also possible (see article on page 24).

## Reference

- [1] *Anisotropy contrast in phonon-enhanced apertureless near-field microscopy using a free-electron laser*, S.C. Kehr, M. Cebula, O. Mieth, T. Härtling, J. Seidel, S. Grafström, L.M. Eng, S. Winnerl, D. Stehr, M. Helm, *Physical Review Letters* 100, 256403 (2008)



# The Dresden High Magnetic Field Laboratory (HLD)

Joachim Wosnitza

The *Hochfeld-Magnetlabor Dresden* (HLD) is a user laboratory that offers a world-unique experimental environment for top-level research in ultrahigh pulsed magnetic fields. After finalizing the lab infrastructure, on schedule and within budget in 2007, the HLD has been accepting proposals for magnet time in the frame of the European infrastructure network EuroMagNET. The available magnetic-field strength of up to 70 T, the versatile and well-adapted experimental infrastructure, and the dedicated local support now attract an ever growing user community. Numerous experimental techniques are available both for in-house research and for users. This includes electrical-transport, magnetization, magnetostriction, ultrasound, and magneto-optical measurements. For the latter, the infrared radiation of the next-door free-electron laser facility ELBE is fed into the pulsed magnets, allowing for unparalleled experiments [1].

Two experiments by Polish and German scientists are exemplary of the growing number of user experiments performed at the HLD by research teams from all over the world. Fig. 1 shows the outcome of a

successful user experiment carried out by a Polish group in 2007, which studied the multiferroic material  $\text{BiFeO}_3$  by pulsed-field magnetization measurements. The coexistence and interdependence of electric and magnetic polarizations in multiferroic materials is of fundamental interest, and their control by either electric or magnetic field makes them good candidates for potential applications. In  $\text{BiFeO}_3$ , the application of large magnetic fields leads to a first-order phase transition, visible in the measured peak-like anomalies in the time-derivative of the magnetization,  $dM/dt$  (Fig. 1). In the high-field phase, the low-field modulated magnetic structure is destroyed most probably which in turn changes the electric polarization in  $\text{BiFeO}_3$  [2].

Another example of a highly sophisticated endeavor is the study of a magnetic-field-induced metal-insulator transition in carbon nanotubes. A group of scientists of the University of Regensburg in cooperation with the HLD succeeded in measuring the electrical resistivity of an individual carbon nanotube as a function of a pulsed magnetic field at low temperatures. Depending on the gate voltage applied to the nanotube, the electrical conductivity could be

switched from metallic to semiconducting behavior by the magnetic field applied along the tube axis (Fig. 2). This field-induced band-gap engineering is a direct consequence of the Aharonov-Bohm effect, i.e. a quantum-interference phenomenon acting on the wavefunction in these quantum-mechanical nano-objects [3].

## References

- [1] See also “Coupling of the free-electron laser facility with pulsed magnetic fields: first results” by S. Zvyagin in this report.
- [2] Magnetization of polycrystalline  $\text{BiFeO}_3$  in high magnetic fields, D. Wardecki<sup>1</sup>, R. Przeniosło<sup>1</sup>, I. Sosnowska<sup>1</sup>, Y. Skourskii, M. Loewenhaupt<sup>2</sup>, Journal of the Physical Society of Japan 77, 103709 (2008)
- [3] Magnetic-field-induced band-gap engineering of carbon nanotubes, S.-H. Jhang<sup>3</sup>, D. Preusche<sup>3</sup>, C. Strunk<sup>3</sup>, Y. Skourskii, in preparation

## Project Partners

- Institute of Experimental Physics, University of Warsaw, Poland<sup>1</sup>
- Institut für Festkörperphysik, Technische Universität Dresden, Germany<sup>2</sup>
- Institut für Experimentelle und Angewandte Physik, Universität Regensburg, Germany<sup>3</sup>

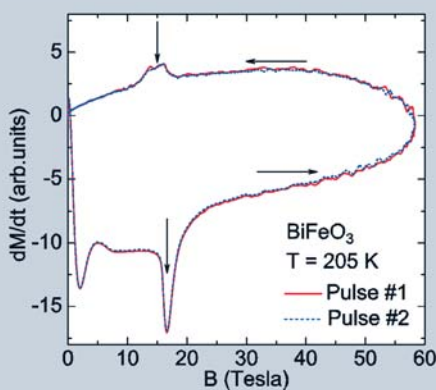


Fig. 1: Field dependence of the induced pick-up coil voltage (proportional to  $dM/dt$ ) for two magnetic-field pulses at 205 K. The horizontal arrows indicate the field-sweep directions. The vertical arrows specify the magnetic transition region.

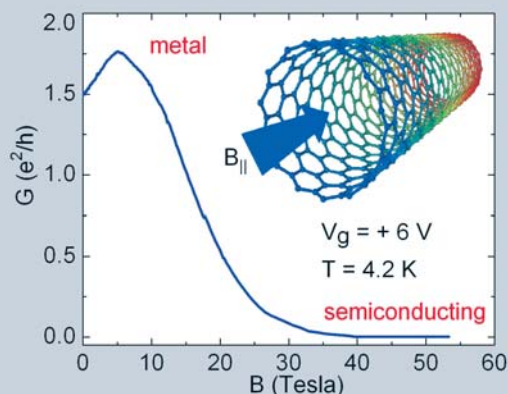
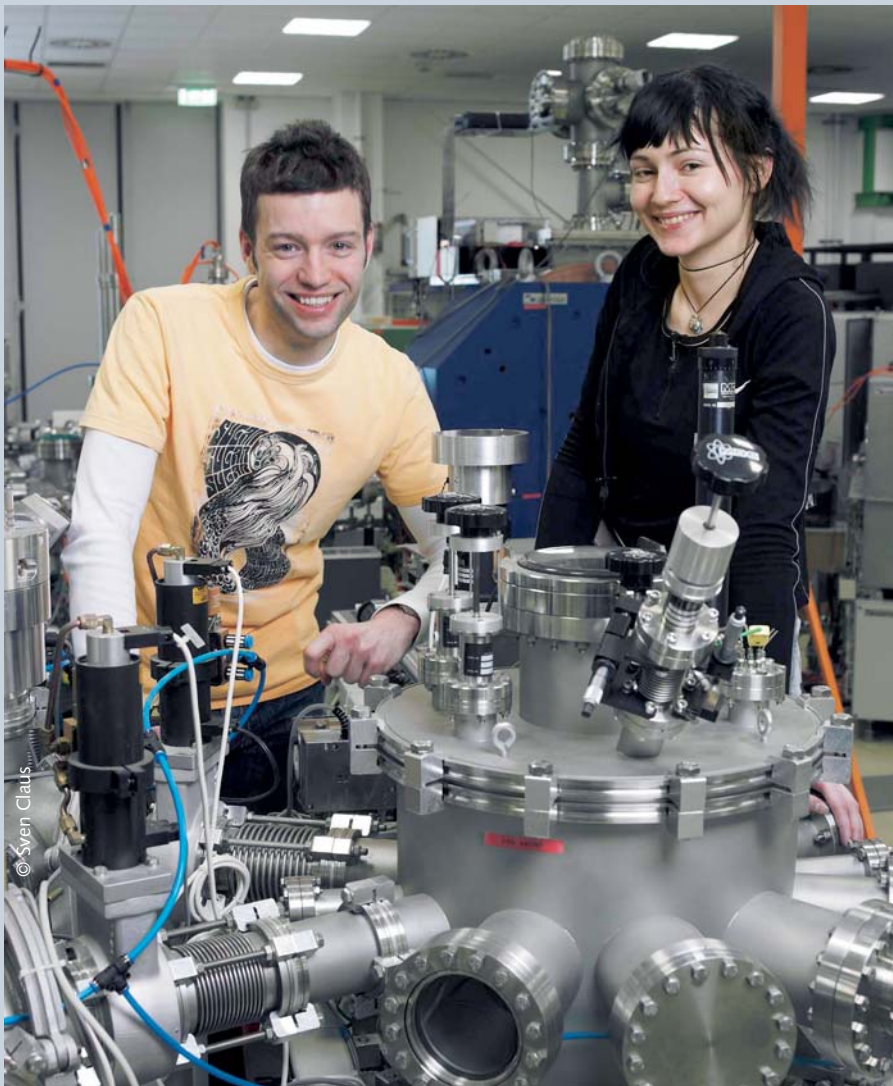


Fig. 2: Field dependence of the electrical conductivity, normalized to the conductance quantum, of an individual nanotube. The magnetic field was aligned along the tube axis (see inset). For the applied gate voltage of 6 V, a field-induced transition from metallic to semiconducting behavior is realized.



# The Ion-Beam Center



Andreas Kolitsch, Wolfhard Möller

The Ion-Beam Center is devoted to the application of ion beams to modify and analyze near-surface layers of materials, and has the status of a European user facility under the name AIM (Application of Ion Beams to Materials Research). The ion-beam center (schematic in Fig. 4, with

the new 6 MV tandetron accelerator) operates three MV electrostatic accelerators, three ion implanters, fine-focused ion-beam devices, highly-charged ion devices, and several experimental installations for plasma immersion ion implantation as well as ion-assisted deposition of thin films. This broad spectrum of ion-beam equipment is

available in the energy range from several eV up to several ten MeV. The main sections of the facility have been installed within the last 15 years and represent world-class quality.

The aim of the research activities at the AIM is to contribute to the development of European materials research by using the diverse possibilities of ion-beam techniques. Basic research to explore new possibilities for surface modification of materials by ion irradiation is combined with the development of technological applications in cooperation with industry.

More than 40 % of user time of AIM devices is made available to external users from universities and other research institutions. About 60 research projects from Germany, stemming from roughly the same number of research groups, benefited from AIM facilities from January 2005 to December 2007. Moreover, 70 groups from the rest of the EU and its associated countries, and 25 groups from other foreign countries, made use of the AIM. Fig. 1 demonstrates the widespread distribution of access in EU countries during this period. A broad spectrum of research topics in microelectronics, electro-optics, semiconductor research, nano-technology, magnetism, mineralogy etc. (see examples [1-7]) are covered as well. In 2008, external users requested use for almost all of the center's experimental facilities including student training (Figs. 2 and 3).

The attraction of the ion-beam center is evidenced by interesting examples of international high-level research performed at the FZD facilities. Recently, a so-called crystal-ion-slicing and bonding technique has been used to fabricate free-standing  $\text{LiNbO}_3$  thin film crystals. The sliced  $\text{LiNbO}_3$



**European user access**

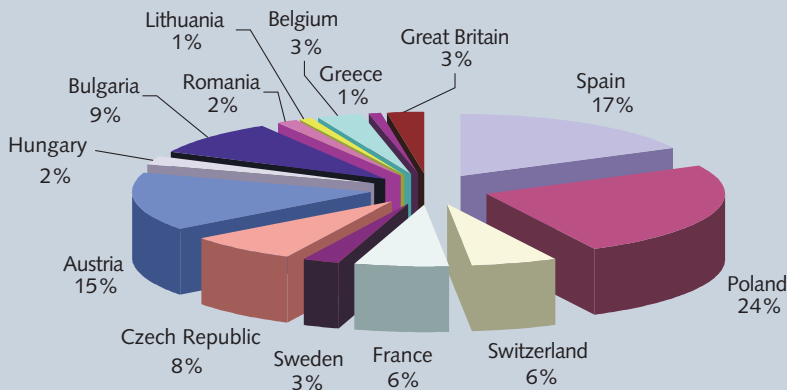


**Fig. 1:** Being a European user facility, the Ion-Beam Center regularly houses guests. Here, the distribution from 2005 till 2007 is shown according to countries.

**Beamtime statistics 2008**

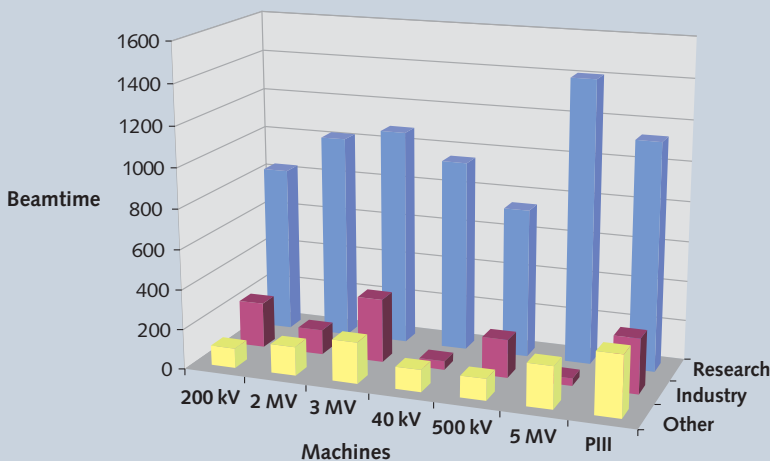


**Fig. 2:** Distribution of beamtime at the Ion-Beam Center in 2008 according to research, industrial, and other purposes.

**Beam statistics - topics**

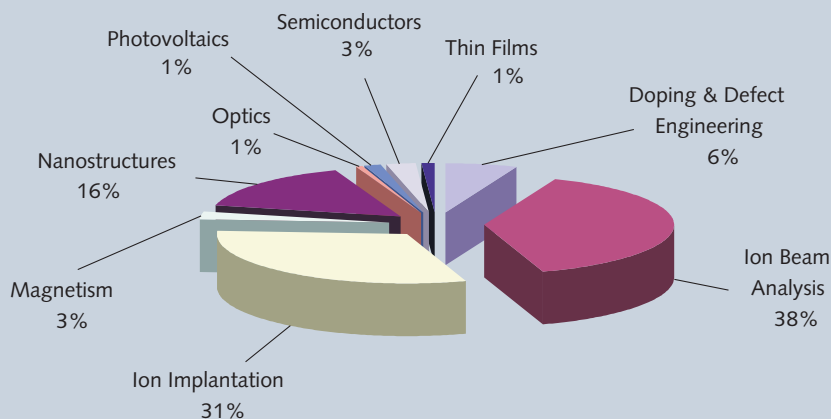


**Fig. 3:** Ion beam analysis and ion implantation are the dominant topics at the Ion-Beam Center.

crystals have very good optical and electro-optical properties comparable to bulk crystals [1]. In the areas of nanomagnetism [4], spintronics, and nanomechanics, one of the main topics of current research is the selective, local generation of ferromagnetism by means of deformation at the micrometer and submicrometer scale of different types of materials, such as ordered intermetallics (e.g. FeAl) or austenitic stainless steel. As another example, switchable two-color Si metal-oxide-semiconductor light emitting diodes containing europium have been fabricated by ion implantation and subsequent annealing processes. During the last years, there was also a high demand for preparation of slow highly-charged-ion induced surface nanostructures on insulating surfaces [7].

The center has continuously expanded its industrial cooperation projects and services. Industry plays an important role through partnerships in cooperative projects utilizing in-house research. From 2005 to 2008, there were direct cooperation projects, along with industrial service provisions, with about 60 groups from German industry and 15 groups from foreign countries. Presently, direct industrial activities account for about 15 % of the capacity of AIM delivered to users. Direct industrial cooperation covers a wide range of industrial research dealing with the development of materials and components, and the characterization of products. These are mainly applied in the semiconductor industry including microelectronics, photovoltaics, tribology, biomaterials, optical coatings, and particle spectroscopy.

From 2009 to 2013, the Ion-Beam Center of the Forschungszentrum Dresden-Rossendorf coordinates the top eleven European ion-beam centers for materials research within the SPIRIT project of the EC, offering integrated infrastructure for European user access and performing joint research activities in the field of ion-solid-interaction.

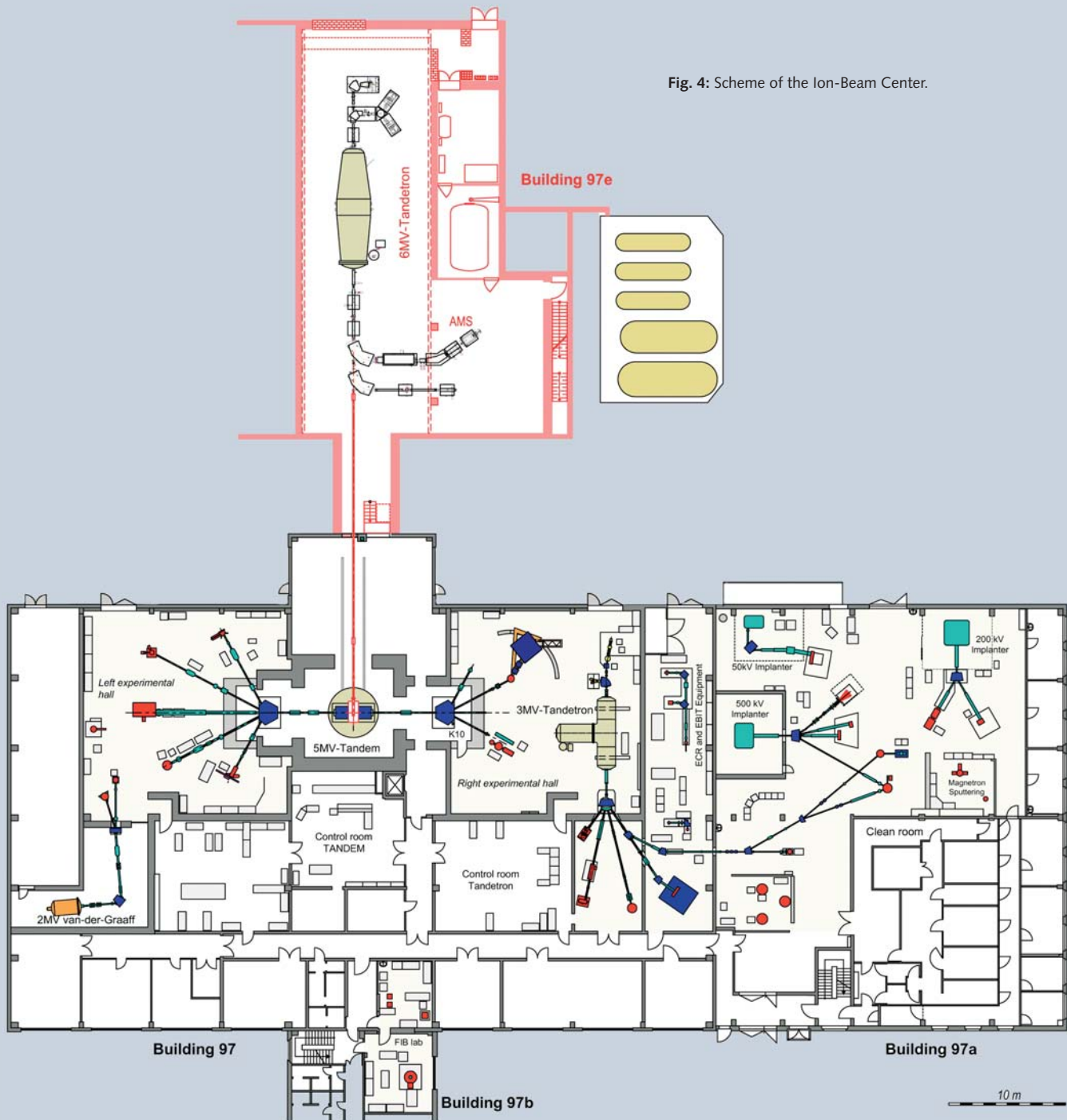


Fig. 4: Scheme of the Ion-Beam Center.

## References

- 1) *Electro-optically tunable microring resonators in lithium niobate*, A. Guarino, G. Poberaj, D. Rezzonico, R. Degl'Innocenti, P. Günter, *Nature Photonics* 1, 407 – 410 (2007)
- 2) *Deviations from Vegard's rule in  $Al_{1-x}In_xN$  (0001) alloy thin films grown by magnetron sputter epitaxy*, T. Seppänen, M. Beckers, U. Kreissig, L. Hultman, J. Birch, *Journal of Applied Physics* 101, 043519 (2007)
- 3) *Effects of irradiation damage on the back-scattering of electrons: silicon-implanted silicon*, L. Nasdala, D. Grambole, A. Kronz, G. Trullenque, *American Mineralogist* 92, 1768 – 1771 (2007)
- 4) *Generation of sub-50 nm magnetic dots by selective irradiation of a paramagnetic intermetallic alloy*, E. Menéndez, J. Sort, M.O. Liedke, J. Fassbender, T. Gemming, A. Weber, L.J. Heyderman, S. Suriñach, K.V. Rao, S.C. Deevi, M.D. Baró, J. Nogués, *Physical Review B* (accepted)
- 5) *Focused ion beam induced synthesis of a porous antimony nanowire network*, C. Schöndorfer, A. Lugstein, Y. Hyun, E. Bertagnolli, L. Bischoff, P.M. Nellen, V. Callegari, P. Pongratz, *Journal of Applied Physics* 102, 044308 (2007)
- 6) *Switchable two-color electroluminescence based on a Si metal-oxide-semiconductor structure doped with Eu*, S. Prucnal, J.M. Sun, W. Skorupa, M. Helm, *Applied Physics Letters* 91, 181121 (2007)
- 7) *Creation of nano-hillocks on  $CaF_2$  surfaces by single slow highly charged ions*, A.S. El-Said, R. Heller, W. Meissl, R. Ritter, S. Facsko, C. Lemell, B. Solleder, I.C. Gebeshuber, G. Betz, M. Toulemonde, W. Möller, J. Burgdörfer, F. Aumayr, *Physival Review Letters* 100, 237601 (2008)

# Materials research with synchrotron radiation at ROBL

Carsten Baehtz, Rui M. S. Martins,  
Shengqiang Zhou, Johannes v. Borany

The Rossendorf Beamline ROBL, operated by the FZD, is a bending magnet beamline (BM20) at the European Synchrotron Radiation Facility (ESRF) in Grenoble, France. The beamline delivers monochromatic X-rays from 6 to 35 keV and is divided into two experimental sections. The first is used for spectroscopic investigation on primarily radioactive samples while the second station is specialized on X-ray diffraction, reflectometry, and scattering experiments for materials research (ROBL-MRH). Additionally, these methods can be combined with small angle scattering or X-ray fluorescence spectroscopy.

The core competence of ROBL-MRH is the analysis of thin films, multilayers, and (ion-beam synthesized) nanostructures. A significant fraction of the experiments are performed as *in-situ* X-ray studies using process chambers for magnetron sputter deposition, ion irradiation, or annealing, respectively. The aim here is to design thin films, near-surface layers, or nanostructures of well-defined features. Non-destructive X-ray analysis *during* materials processing is applied to characterize the surface, film, or interface properties via measuring thickness, roughness, and density. Furthermore, the formation or transformation of crystalline phases, their texture as well as strain and stress state can be determined. These data are the key to understand the underlying physical or chemical processes and to interpret the corresponding macroscopic materials properties. The following studies demonstrate the capabilities of ROBL-MRH.

## *In-situ* investigations – watching the action

Ni-Ti Shape Memory Alloys are smart materials undergoing so-called first-order martensitic transformations driven by temperature and/or stress. In the form of films, especially with a gradient in composition along the film thickness, they are very attractive candidates for microelectro-mechanical system applications. Such films have been deposited by magnetron co-sputtering, exhibiting distinct composition and microstructure along the growth direction. This *in-situ* study has been useful for optimizing deposition parameters in order to fabricate films with a two-way reversible actuation. The chosen sequence and amount of co-sputtering led to different peak intensities of various phases (Fig. 1) [1]. Starting with an equiatomic composition the B2 phase stacked onto (h00) planes on the naturally oxidized

Si(100) substrate. An increase of the Ti content up to 60 % led to the  $\text{Ti}_2\text{Ni}$  phase. By stopping the Ti co-sputtering,  $\text{Ti}_2\text{Ni}$  dissolved and, thus, took the role of a Ti reservoir for the formation of B2 phase now preferentially stacking onto (110), the more densely packed crystallographic plane. The evolution of the lattice parameter obtained from the different diffraction peaks gave an important indication of the intermediate biaxial stress state of the Ni-Ti films [2].

## Simultaneous structural and electrical characterization of GST films

One of the emerging concepts for non-volatile memories, e.g. for solid state discs, makes use of the fact that in some chalcogenides, e.g.  $\text{Ge}_2\text{Sb}_2\text{Te}_5$  (GST), an amorphous-crystalline phase transition is associated with a dramatic change of the electrical resistivity [3]. The information bit in so-called Phase Change Memories

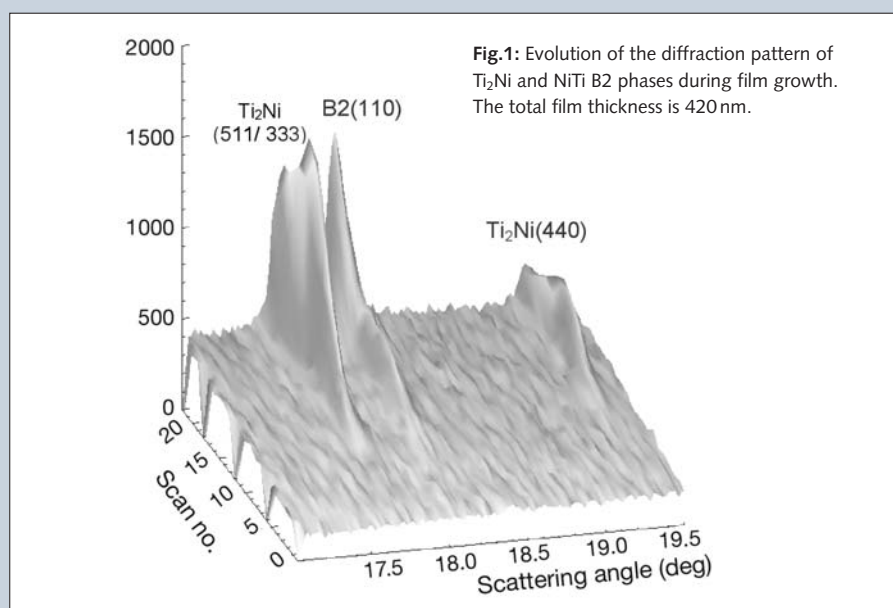
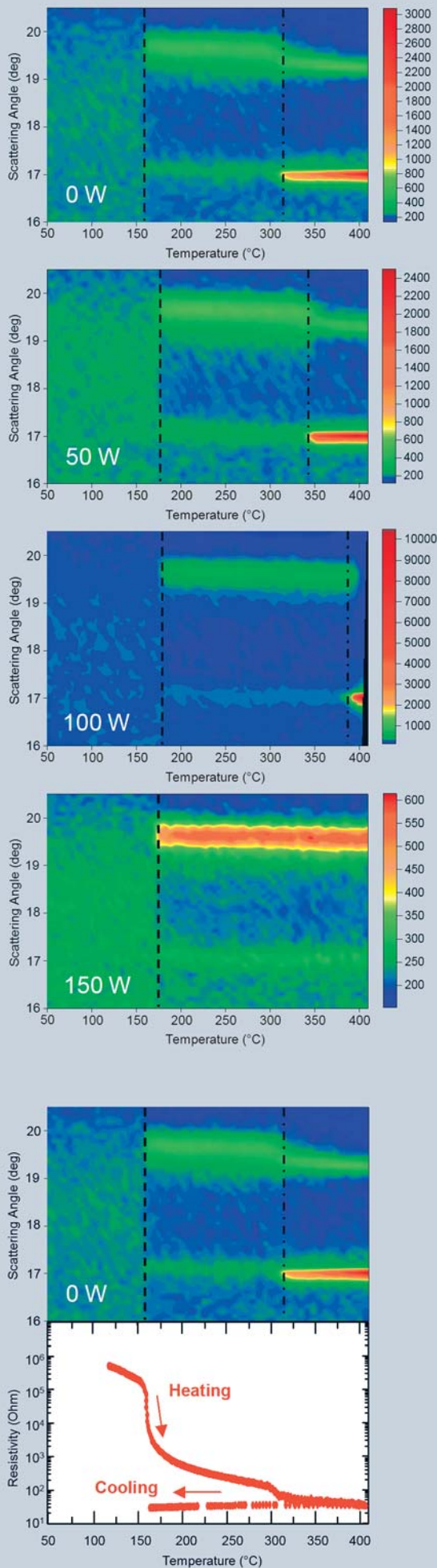


Fig.1: Evolution of the diffraction pattern of  $\text{Ti}_2\text{Ni}$  and NiTi B2 phases during film growth. The total film thickness is 420 nm.



**Fig. 2:** (a) Colour maps of temperature dependent XRD measurements of SiO<sub>2</sub> doped GST films (from top to bottom with increasing SiO<sub>2</sub> content indicated by increasing power).

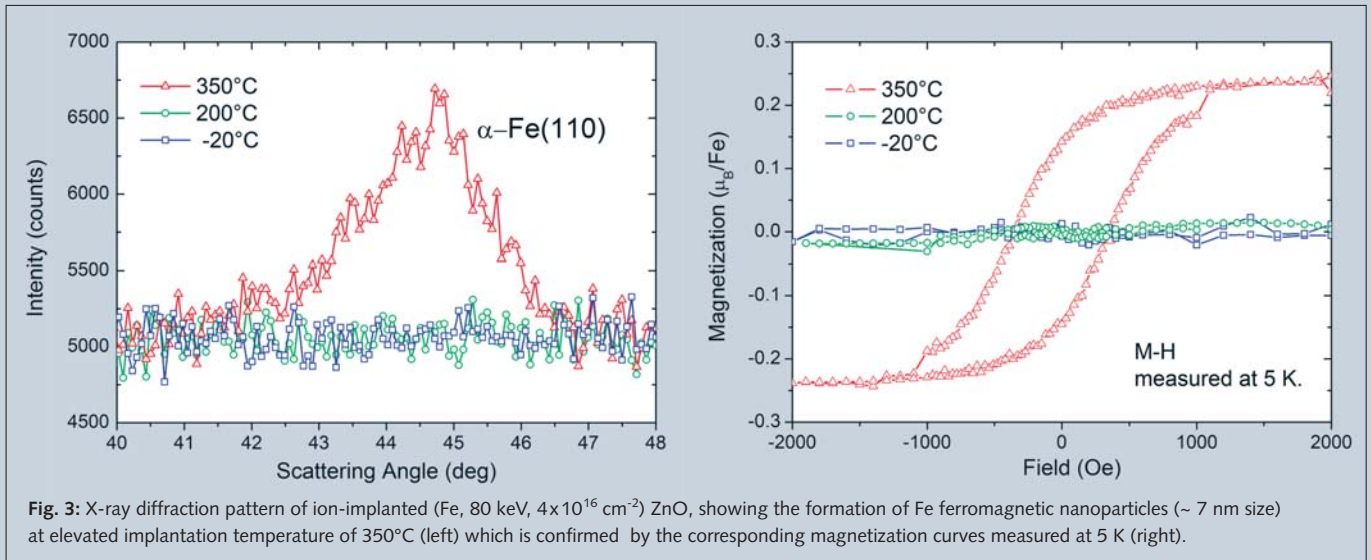
(b) Simultaneous measurement of structural and electrical properties, the resistance drops significantly upon phase change.

(PCM) is stored defining 1 as amorphous state (high resistivity) and 0 as crystalline state (low resistivity). The alteration between amorphous (a) and crystalline (c) state is realized by current or laser pulses of different intensity and/or duration, which result either in local heating (a → c) or local melting / fast quenching (c → a). By using dopants (e.g. Si, SiO<sub>2</sub>, N...), the melting and crystallization temperature can be optimized according to the technological demands.

Initiated by cooperation with Qimonda Dresden, a series of SiO<sub>2</sub>-doped GST films has been investigated at ROBL by means of high-temperature X-ray diffraction combined with simultaneous measurement of the electrical resistance using four-point-probe. All GST films were amorphous after deposition. During annealing with a constant temperature rate of 5 K/min, the diffraction pattern clearly revealed a first phase change from amorphous to crystalline cubic phase found in the range between 150°C and 200°C, depending on the SiO<sub>2</sub> content in the film. A second phase transition from cubic to hexagonal phase was found in the range between 300°C and 390°C only for samples with low SiO<sub>2</sub> concentration (Fig. 2a). Simultaneous electrical measurements revealed the drastic decline (about two orders) in resistance correlating with the first phase transition (Fig. 2b). A further decline was observed during the cubic-hexagonal transition. Such investigations deliver significant data for the crystallization kinetics and the technological optimization of the film composition.

### Correlation of structural and materials properties

Also, *ex-situ* investigations performed at ROBL-MRH show that diffraction techniques are an adequate method to correlate structural parameters and materials properties. In the field of diluted magnetic semiconductors, like Fe in ZnO [4], the phase formation was monitored. Iron was incorporated into single crystalline ZnO by ion implantation. At fluences below  $2 \times 10^{16} \text{ cm}^{-2}$  no crystalline iron was observed after implantation at room temperature, at higher fluences and temperatures above 200 °C non-textured,



nano-sized  $\alpha$ -Fe crystallites were detected (Fig. 3). Post-synthesis annealing leads to a growth of the crystallites. The correlation of the structural investigation with magnetic measurements directly shows that ferromagnetism in transition-metal-doped ZnO often originates from metal nanoparticles, which precipitate during materials processing [4, 5].

These examples show that X-ray diffraction and scattering methods are powerful tools to elucidate structural and crystallographic characteristics and correlate them with macroscopic materials properties. We are convinced that, in the future, especially the *in-situ* techniques in combination with complementary methods will gain even more importance.

#### References

- [1] *Study of graded Ni-Ti shape memory alloy film growth on Si(100) substrate*, R.M.S. Martins, N. Schell, A. Mücklich, H. Reuther, M. Beckers, R.J.C. Silva<sup>1</sup>, L. Pereira<sup>1</sup>, F.M. Braz Fernandes<sup>1</sup>, Applied Physics A 91, 291 (2008)
- [2] *Characterization of Ni-Ti (shape memory alloy) thin film by in-situ XRD and complementary ex-situ techniques*, R.M.S. Martins, N. Schell, H. Reuther, L. Pereira<sup>1</sup>, R.J.C. Silva<sup>1</sup>, K.K. Mahesh<sup>1</sup>, F.M. Braz Fernandes<sup>1</sup>, Materials Science Forum 587, 672 (2008)
- [3] *Phase-change materials for rewritable data storage*, M. Wuttig, N. Yamada, Nature Materials 6, 824 (2007)
- [4] *Fe-implanted ZnO: Magnetic precipitates versus dilution*, S. Zhou, K. Potzger, G. Talut, H. Reuther, J. von Borany, R. Grötzschel, W. Skorupa, M. Helm, J. Fassbender, N. Volbers, M. Lorenz, T. Herrmannsdörfer, Journal of Applied Physics 103, 023902 (2008)
- [5] *Crystallographically oriented Co and Ni nanocrystals inside ZnO formed by ion implantation and postannealing*, S. Zhou, K. Potzger, J. von Borany, R. Grötzschel, W. Skorupa, M. Helm, J. Fassbender, Physical Review B 77, 035209 (2008)

#### Project Partners

- CENIMAT Center of Investigations of Materials, Faculty of Sciences and Technology, New University of Lisbon, Monte de Caparica, Portugal<sup>1</sup>
- Qimonda Dresden GmbH & Co. OHG, Dresden, Germany

## RESEARCH

# Magnetic control of temperature fluctuations in crystal growth processes



Ilmars Grants, Gunter Gerbeth

Single crystals of silicon or gallium arsenide (GaAs) are today mainly produced by means of the so-called Czochralski technique, as it is sketched in Fig. 2. A seed crystal is touched to the free surface of the semiconductor melt, and a single crystal grows when the seed is slowly pulled upwards. In order to improve the axial symmetry of the crystal, both the crucible and the crystal rotate in opposite directions with typically 5 and 10 rpm, respectively. The crucible is typically a factor of 3 larger in diameter than the crystal. Today, commercially grown silicon crystals have standard diameters of 300 mm (see Fig. 1), though sizes of 200 mm are still in production and larger sizes of up to 450 mm have already been achieved.

The temperature of the crystal-melt interface is the melting temperature of the material, for silicon 1414°C. The temperature of the melt in the crucible is some 10 to 20 degrees higher as all the melt should be kept in the molten state. Due to the size of the crucible, there are rather strong motions in the melt caused by buoyancy, crucible/crystal rotations, and thermocapillarity at the free surface of the melt. These motions are turbulent, thus causing also fluctuations of the temperature. One of the basic challenges for crystal growth is the limitation of temperature fluctuations at the crystal-melt interface. If, for instance, those fluctuations were in the range of several degrees Kelvin, the crystal would not grow in a continuous way. Instead, a period of crystallization would be followed by a remelting of parts of the crystal, and all this in a turbulent, thus temporally irregular way. Obviously, this is not good for the crystal quality. In fact, the acceptable temperature

Fig. 1: A 300 mm silicon crystal grown by the Czochralski crystal growth process, picture by Siltronic AG.

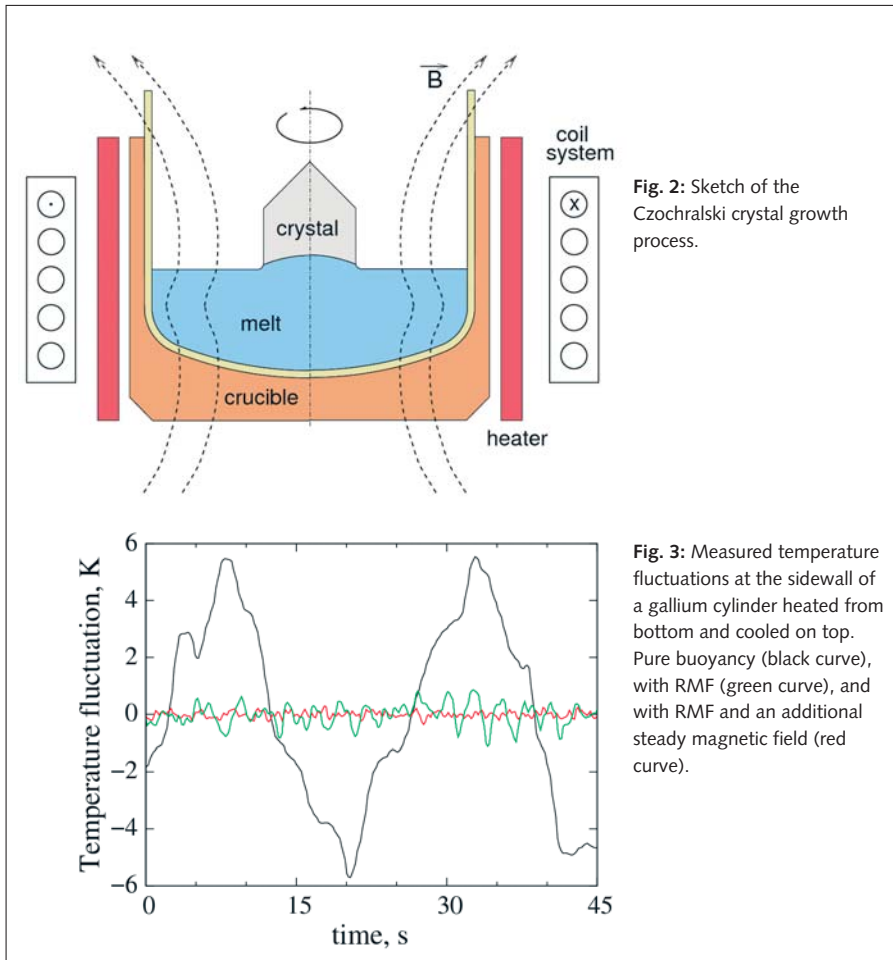


Fig. 2: Sketch of the Czochralski crystal growth process.

Fig. 3: Measured temperature fluctuations at the sidewall of a gallium cylinder heated from bottom and cooled on top. Pure buoyancy (black curve), with RMF (green curve), and with RMF and an additional steady magnetic field (red curve).

fluctuations are the reason why the initial height of the melt is limited to less than half of the crucible diameter, as sketched in Fig. 2. From an economical point of view, a much larger melt height is desirable since larger sized or longer crystals could be obtained from the growth process. For larger initial melt heights, however, the turbulent temperature fluctuations increase to an unacceptable level.

Such temperature fluctuations can effectively be reduced by applying a rotating magnetic field (RMF), which

primarily produces an azimuthal rotation of the melt. At first sight, this seems similar to the mechanical rotation of the crucible or crystal, but the resulting melt flow differs strongly since the RMF acts with a force field distributed over the whole melt volume, whereas the rotating crucible/crystal just gives shear at the melt boundaries. In a series of model experiments [1, 2], we have shown how the RMF affects the temperature fluctuations in a melt. For the model experiments, low-melting gallium ( $T_m = 29^\circ\text{C}$ ) was used as it allows to measure the interesting flow velocities

and temperatures. If the RMF is strong enough, the melt motion changes qualitatively from a large-scale low-frequency turbulence to a small-scale high-frequency turbulence. The measured temperature signal is shown in Fig. 3. The pure buoyancy convection produces fluctuations of  $\pm 6\text{ K}$ , which is certainly too high for crystal growth. The RMF reduces this fluctuation level drastically. A superimposed steady magnetic field reduces the fluctuations even further. Fluctuations of less than  $\pm 1\text{ K}$  are known to be no serious problem for the growth process. Surprisingly, the necessary RMF strength remains very low. For a realistic 120 kg initial GaAs load in a 30 cm crucible, the magnetic field is less than 1 mT.

In conclusion, a very efficient method for reducing temperature fluctuations, which allows starting Czochralski crystal growth processes with much larger initial melt heights, has been demonstrated experimentally. A patent has been filed on this method [3].

#### References

- [1] *Experimental study of the suppression of Rayleigh—Benard instability in a cylinder by combined rotating and static magnetic fields*, I. Grants, A. Pedchenko, G. Gerbeth, *Physics of Fluids* 18, 124104 (2006)
- [2] *The suppression of temperature fluctuations by a rotating magnetic field in a high aspect ratio Czochralski configuration*, I. Grants, G. Gerbeth, *Journal of Crystal Growth* 308, 290 – 296 (2007)
- [3] I. Grants, G. Gerbeth, *Deutsches Patentamt*, DE 10 2007 036944.3

#### Collaborations

- DFG Collaborative Research Center SFB 609, Technische Universität Dresden, Germany
- Institute of Physics Riga, Latvia

## An exotic high-field state of superconductivity



Beate Bergk, Joachim Wosnitza

For superconductors, usually high magnetic fields are detrimental to the superconducting state, since they turn the material into a normal conductor. However, for some materials, a new superconducting hybrid phase between the normal and the superconducting state is predicted to occur in high magnetic fields and at low temperatures. In this phase, parts of the material stay superconducting whereas other parts turn into the normal conducting state. Due to this hybrid state, the superconductivity can survive even at very high magnetic fields. This state preferably appears in stacked materials that consist of ultra-thin conducting and insulating layers.

P. Fulde and R. Ferrell predicted the existence of this special superconducting state already in 1964 [1]. At about the same time, two other researchers independently predicted the same phase [2], which is therefore called Fulde-Ferrell-Larkin-Ovchinnikov (FFLO) state. It is characterized by a spatial modulation of the superconductivity along the direction of the applied magnetic field. At high magnetic fields, the magnetic, or Zeeman energy, eventually destroys superconductivity. Under certain circumstances, however, two electrons with opposite spin may still couple to a Cooper pair so that the momenta of the two electrons are no longer equal, as it is at lower applied field. Consequently, the Cooper pair in the FFLO state has a finite momentum, corres-

ponding to a wavevector or oscillating amplitude, i.e. a spatial modulation.

Good candidates for exhibiting the FFLO state are quasi-two-dimensional layered superconductors, especially organic superconductors. High-quality single crystals of such molecular materials are well characterized, have been studied for many years, and show a plethora of fascinating phenomena [3]. A well-known family of quasi-two-dimensional organic metals and superconductors is based on the molecule bisethylenedithio-tetra-thiafulvalene (BEDT-TTF or ET for short), with ET molecules forming highly conducting layers that are separated by 'insulating' anion layers. Here, novel specific-heat experiments of the organic



superconductor  $\kappa$ -(BEDT-TTF)<sub>2</sub>Cu(NCS)<sub>2</sub> have been performed by applying the external magnetic field exactly parallel to the conducting ET layers.

The specific heat, measured in static magnetic fields at the Grenoble High Magnetic Field Laboratory, clearly shows two sharp anomalies at low temperatures and high magnetic fields (Fig. 1). The lower transition is of first order and, therefore, shows a well resolvable temperature hysteresis ( $\sim 0.05$  K at 22 T) while the main superconducting transition develops only a small hysteresis of less than 0.02 K (inset of Fig. 1). This proves the existence of an additional thermodynamic phase within the superconducting state, i.e. the FFLO state, most probably.

Given its known parameters,  $\kappa$ -(BEDT-TTF)<sub>2</sub>Cu(NCS)<sub>2</sub> was expected to become a normal conductor at about 22 Tesla. But if the magnetic field is applied parallel to the organic-molecule layers, the superconductivity can survive also in much higher fields due to the formation of the hybrid phase. Recently, in a second series of experiments utilizing high-field magnetization measurements, the FFLO phase was investigated in more detail towards higher magnetic fields and lower temperatures. As a result, it was possible to observe superconductivity of that material in high magnetic fields up to 32 Tesla. The resulting schematic phase diagram is shown in Fig. 2.

The investigation was a joint effort between scientists of the Universities of Geneva/Switzerland, Braunschweig/Germany, Osaka/Japan, and of the Grenoble High Magnetic Field Laboratory in France, as well as of the Dresden High Magnetic Field Laboratory (HLD) of the FZD. In order to better understand this long-time predicted, but only recently found fascinating state of matter, researchers at the HLD are currently preparing further collaborative investigations, also on other organic superconductors.

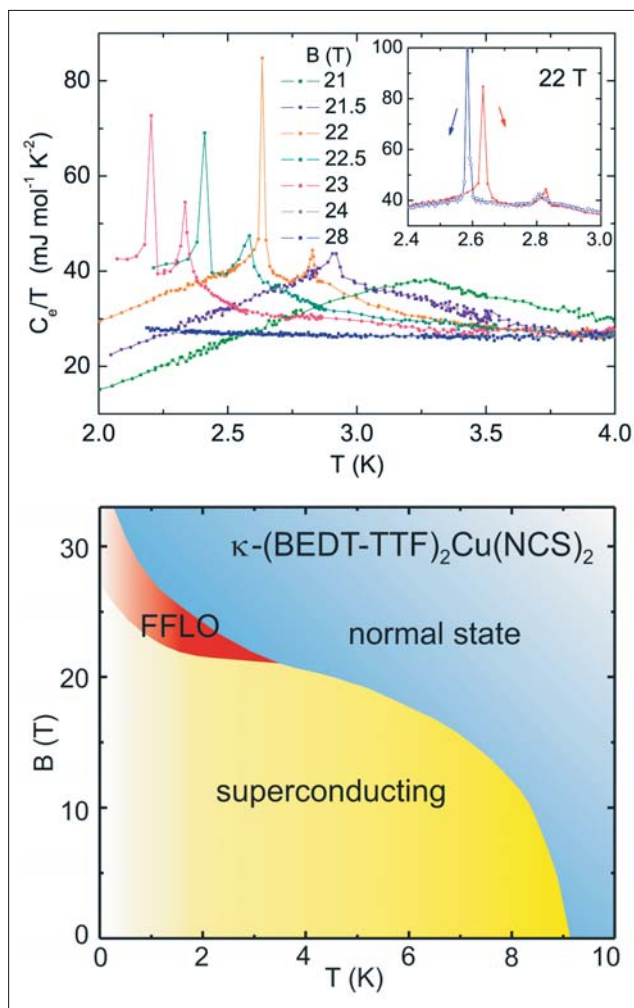


Fig. 1: Temperature dependence of the electronic contribution to the specific heat,  $C_e/T$ , of  $\kappa$ -(BEDT-TTF)<sub>2</sub>Cu(NCS)<sub>2</sub> in magnetic fields applied parallel to the superconducting layers.

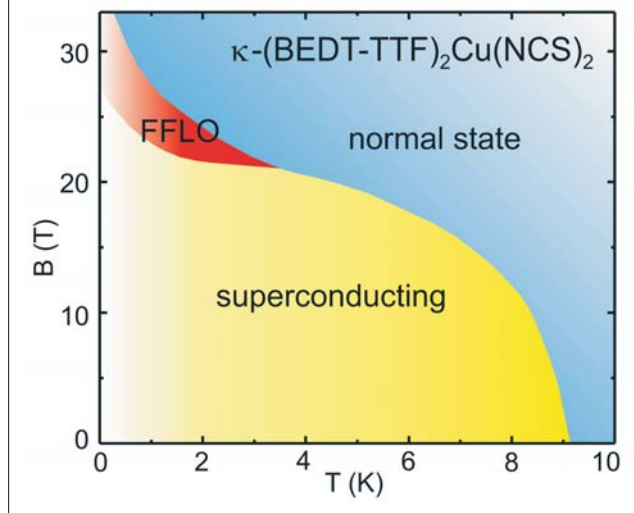


Fig. 2: Schematic phase diagram of the organic superconductor  $\kappa$ -(BEDT-TTF)<sub>2</sub>Cu(NCS)<sub>2</sub>. At low temperatures and high magnetic fields the Fulde-Ferrell-Larkin-Ovchinnikov-Phase (FFLO) occurs. In the diagram it is visible as the red interspace.

#### References

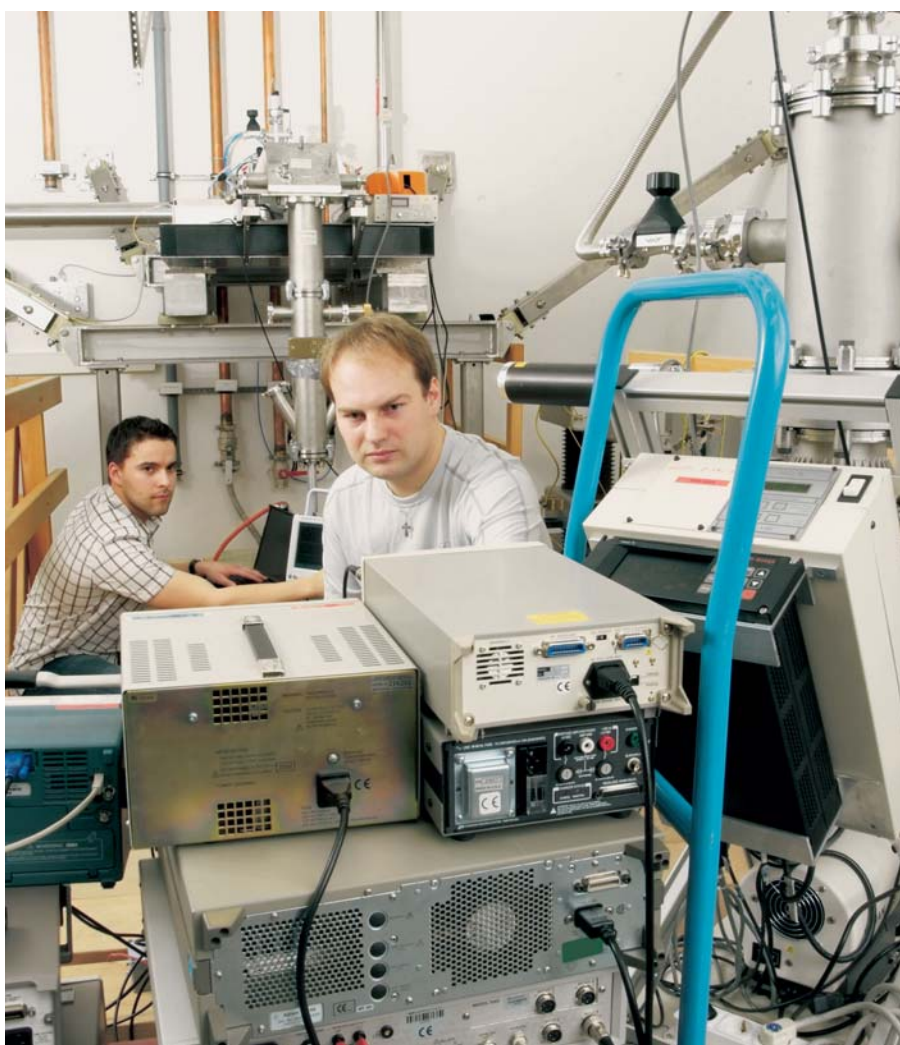
- [1] *Superconductivity in a strong spin-exchange field*, P. Fulde, R.A. Ferrell, Physical Review Letters 135, A 550 (1964)
- [2] *Nonuniform state of superconductors*, A.I. Larkin, Y.N. Ovchinnikov, Žurnal éksperimental'noj i teoretičeskoj fiziki (Zh. Eksp. Teor. Fiz.) 47, 1136 (1964) [Sov. Phys. JETP 20, 762 (1965)]
- [3] *Unconventional Superconductivity in Novel Materials*, M.B. Maple<sup>1</sup>, E.D. Bauer<sup>1</sup>, V. Zapf<sup>1</sup>, J. Wosnitza, in: *Superconductivity – Conventional and Unconventional Superconductors*, Vol. 1, edited by K.H. Bennemann and J.B. Ketterson, Springer, Berlin, 2008, p. 639 – 762
- [4] *Calorimetric evidence for a Fulde-Ferrell-Larkin-Ovchinnikov superconducting state in the layered organic*

*superconductor*  $\kappa$ -(BEDT-TTF)<sub>2</sub>Cu(NCS)<sub>2</sub>, R. Lortz<sup>2</sup>, Y. Wang<sup>3</sup>, A. Demuer<sup>3</sup>, P.H.M. Böttger, B. Bergk, G. Zwicknagl<sup>4</sup>, Y. Nakazawa<sup>5</sup>, J. Wosnitza, Physical Review Letters 99, 187002 (2007)

#### Project partners

- Department of Physics and Institute for Pure and Applied Physical Sciences, University of California, San Diego La Jolla, California, USA<sup>1</sup>
- Physics Department, Hong Kong University of Science & Technology, Hong Kong<sup>2</sup>
- Grenoble High Magnetic Field Laboratory, CNRS, Grenoble, France<sup>3</sup>
- Institut für Mathematische Physik, Technische Universität Braunschweig, Germany<sup>4</sup>
- Department of Chemistry, Osaka University, Japan<sup>5</sup>

## Coupling of the free-electron laser facility with pulsed magnetic fields: first results



Sergei Zvyagin

At the FZD, the truly unique combination of the free-electron-laser (FEL) facility at ELBE with the ultrahigh magnetic fields of the Dresden High Magnetic Field Laboratory (HLD) allows to perform unprecedented novel magneto-optical and resonance experiments. These large-scale facilities are adjacent to one another and

are connected via a beamline from the free-electron lasers to the pulsed magnets of the HLD. In a collaborative effort between the Institute of Radiation Physics, the Institute of Ion Beam Physics and Materials Research, the Central Technology Department, and the HLD, the beamline was completed and successfully put into operation in 2007. In the continuous-wave (CW) mode the FELs generate high-power

(up to several 10 Watts) radiation in the wavelength range between 4 and 250  $\mu\text{m}$  (corresponding to 1.2 – 75 GHz), which allows for a wide range of experiments in the mid- and far-infrared spectral range in high magnetic fields, not possible so far. Here, we present two scientific results obtained by use of this worldwide unmatched facility.

### Magneto-optical studies in semiconductors

As one of the first investigations, a systematic study of the cyclotron-resonance (CR) absorption of the two-dimensional charge carriers (holes in this case) in strained InGaAs/GaAs quantum wells in the quantum limit was performed. Such kinds of nanostructured semiconductor devices are of great interest for many potential applications, like high-frequency electronics, solar cells, and lasers. By using either semiconductor quantum-cascade lasers or different frequencies supplied by the FELs, clear cyclotron-resonance absorption dips could be resolved in the transmission signals (Fig. 1). The energies of cyclotron-resonance transitions could be traced as a function of magnetic field up to 55 T. A nonlinear shift of the cyclotron-resonance lines with increasing magnetic field and a remarkable CR line splitting for fields above 20 T was evidenced. This behavior can be excellently described by taking into account the non-parabolic quantum-well potential and an appropriate strain profile [1].

### Electron spin resonance with infrared radiation

In 2007, a sophisticated experimental infrastructure for measuring electron spin resonance (ESR) in high magnetic fields was put into operation at the HLD. This technique is a powerful tool for investi-

gating low-energy excitation spectra, especially in magnetic materials. The novel experimental approach (called tunable-frequency ESR) pursued at the HLD is of particular importance for studying magnetic excitation spectra in materials exhibiting field-induced phenomena (including magnetic phase transitions) and spin systems with a very large zero-field splitting. The available equipment allows for ESR experiments in the sub-THz and THz frequency range in pulsed magnetic fields up to 60 T and beyond. Towards lower frequencies, the radiation of backward wave oscillators and tunable semiconductor sources with mm-wavelength radiation extends the accessible frequency range down to 30 GHz. The highest frequency of about 1.3 THz supplied by these devices fits nicely with the lower-frequency range of the ELBE FELs. This world-unique setup, therefore, places no restrictions in the challenging THz range, i.e. it has closed the so-called 'THz gap'. The result of one of the first pulsed-field ESR experiments performed by use of the infrared radiation of the FEL is shown in Fig. 2. Here, the magnetically low-dimensional organic material  $(C_6H_9N_2)CuCl_3$  was investigated. Clear and sharp ESR absorption dips are visible during the up and down sweep of the magnetic-field pulse at 44 T.

Both experimental setups are now available for users and allow unparalleled cyclotron-resonance and ESR experiments to be performed at the HLD.

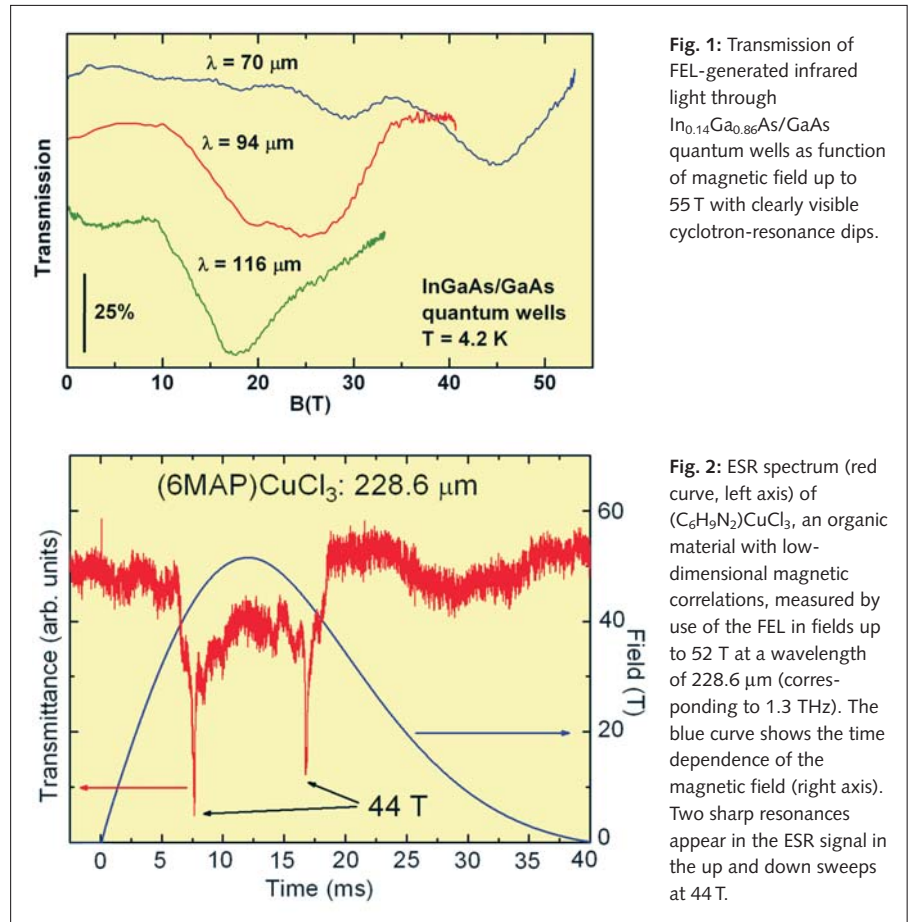


**Fig. 1:** Transmission of FEL-generated infrared light through  $In_{0.14}Ga_{0.86}As/GaAs$  quantum wells as function of magnetic field up to 55 T with clearly visible cyclotron-resonance dips.

**Fig. 2:** ESR spectrum (red curve, left axis) of  $(C_6H_9N_2)CuCl_3$ , an organic material with low-dimensional magnetic correlations, measured by use of the FEL in fields up to 52 T at a wavelength of 228.6  $\mu m$  (corresponding to 1.3 THz). The blue curve shows the time dependence of the magnetic field (right axis). Two sharp resonances appear in the ESR signal in the up and down sweeps at 44 T.

#### References

- [1] *High-field splitting of the cyclotron resonance absorption in strained p-InGaAs/GaAs quantum wells*, O. Drachenko, D.V. Kozlov<sup>1</sup>, V.Ya. Aleshkin, V.I. Gavrilenko<sup>1</sup>, K.V. Maremyanin<sup>1</sup>, A.V. Ikonnikov<sup>1</sup>, B.N. Zvonkov<sup>2</sup>, M. Goiran<sup>3</sup>, J. Leotin, G. Fasching, S. Winnerl, H. Schneider, J. Wosnitza, M. Helm, *Physical Review B* 79, 073301 (2009)
- [2] *THz-range free-electron laser ESR spectroscopy: techniques and applications in high magnetic fields*, S.A. Zvyagin,

M. Ozerov, E. Čížmár, D. Kamensky, S. Zherlitsyn, T. Herrmannsdörfer, J. Wosnitza, R. Wunsch, W. Seidel, submitted to *Review of Scientific Instruments*

#### Project partners

- Institute for Physics of Microstructures RAS, Nizhny Novgorod, Russia<sup>1</sup>
- N.I.Lobachevsky State University of Nizhny Novgorod, Physico-Technical Research Institute, Nizhny Novgorod, Russia<sup>2</sup>
- Laboratoire Nationale des Champs Magnétiques Pulsés, Toulouse, France<sup>3</sup>

# Superconductivity in doped semiconductors

Thomas Herrmannsdörfer, Viton Heera

In recent years, two investigations on elemental semiconductors, diamond and silicon, have considerably inspired the scientific community, although or because these studies have gone well beyond the classical terrain of semiconductor physics. Two research groups have surprised the community with their findings that boron-doped diamond and silicon can undergo a transition to a superconducting ground state [1, 2]. Although superconductivity has been observed in several doped binary semiconductors over the years, it has not been seen in the simple elemental representatives at ambient pressure conditions before.

For a deeper insight into the Cooper-pairing mechanism of doped elemental superconductors, investigations on highly doped semiconductors have started at the FZD as a joint effort between the Rossendorf Ion-Beam Center and the Dresden High Magnetic Field Laboratory (HLD). In particular, we aimed at observing superconductivity in the third elemental group-IV semiconductor, germanium, and started to investigate superconductivity of doped diamonds in more detail. Thanks to the expertise in material processing at the Ion-Beam Center of the FZD and at the University of Bayreuth, one of our external project partners, we have been able to investigate highly pure and well characterized samples, most likely unrivalled in quality so far.

In order to transform a semiconductor into a superconductor, heavy p-type doping well above the metal-insulator transition is required. Otherwise the charge-carrier density of these materials is too low to create a superconducting state at low temperatures. Our partners of the University of Bayreuth were able to produce boron-doped diamonds by using a large-volume multi-anvil 5000-ton press. We identified them as superconductors with a transition temperature of about 2 K by means of electrical-transport and heat-capacity experiments performed at the HLD. The observed large isotope effect is strong evidence of a conventional electron-phonon coupling mechanism in these superconductors, i.e. lattice vibrations (phonons) are responsible for

**Fig. 1:** Microstructure of boron-doped superconducting diamond investigated by high-resolution transmission-electron microscopy. The picture displays the complex nonhomogeneous distribution of boron in the sample which was manufactured using a high-temperature high-pressure process.

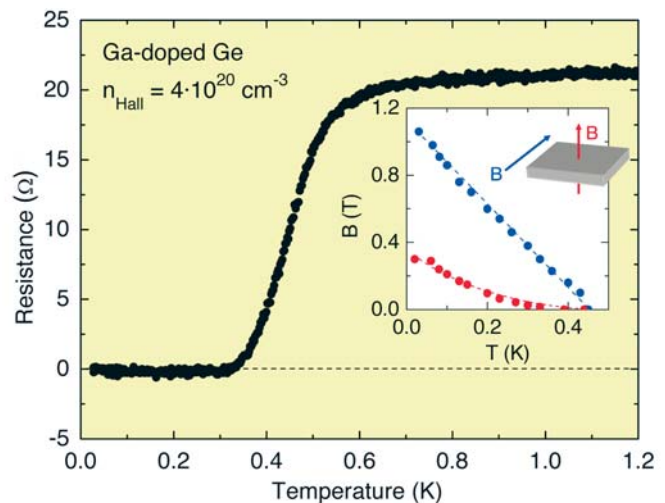
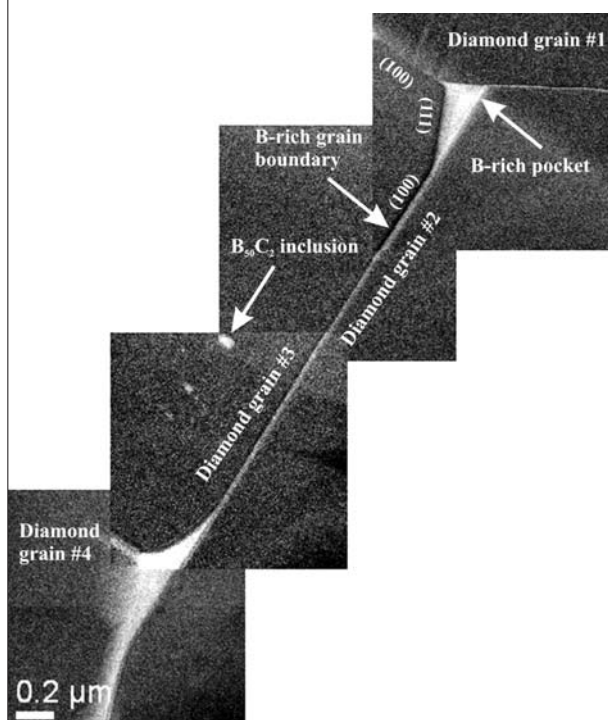


**Fig. 2:** Resistive superconducting transition of a Ga-doped Ge sample observed in zero field. The flash-lamp annealing at a fluence of  $50.8 \text{ J/cm}^2$  has caused a Hall carrier concentration of about  $4 \cdot 10^{20} \text{ cm}^{-3}$  in the Ga-doped Ge layer having an effective thickness of 60 nm. The two-dimensional character of the thin-film superconductor can be clearly seen in the magnetic field – temperature phase diagram (see inset). Critical fields applied parallel to the Ga-doped Ge layer are considerably larger (blue) than perpendicular to the plane (red).

the attractive interactions between Cooper-paired electrons. However, analyzing the polycrystalline samples on the microscopic scale by high-resolution transmission-electron microscopy, we found that amorphous boron-rich intergranular layers and pockets in the framework of  $\mu\text{m}$ -sized diamond crystallites (see Fig. 1) are most likely responsible for superconductivity [3]. That is, instead of boron-doped diamond, carbon-doped boron most probably is the superconducting phase in these samples. This finding is consistent with our observation that diamonds doped by ion implantation do not undergo superconductivity [4].

Germanium (Ge) has been considered as the least likely candidate for superconductivity among the three elemental group-IV semiconductors. Creating an adequate doping level by proper sample preparation plays a decisive role here, even more than in diamond and silicon. Using gallium (Ga) atoms, we have succeeded in achieving a doping level of charge carriers ( $\sim 10^{21}\text{cm}^{-3}$ ) which is large enough to form a condensate of Cooper pairs in Ge. For this, we employed high-dose Ga-ion implantation (up to 8 % Ga in a 60 nm thin Ge layer) and subsequently annealed the layer (specimen) by short-time flash-lamp heating on the millisecond timescale. Indeed, this procedure allowed us to observe superconductivity in Ga-doped Ge, i.e. in one of the few remaining 'islands of the periodic table of elements' in which superconductivity had not been found so far [5]. Under suitable preparation conditions, superconductivity occurs in Ge:Ga for temperatures below 0.5 K and ambient pressure (Fig. 2). This sheds a new light on doped elemental semiconductors, and Ga-doped Ge might even serve as superconducting model system as it allows for a well-controlled

tuning of its superconducting parameters via modification of its hole concentration. The combination of ion implantation and subsequent flash-lamp annealing can be employed to fabricate well defined thin-layer superconductors with reproducible electrical-transport properties. The thin-layer structure of our Ge:Ga samples causes their extraordinary large and anisotropic critical magnetic fields for superconductivity (see inset of Fig. 1). Although the critical temperatures of Ga-doped Ge samples are far below those of high-temperature superconductors, there is a qualitative relationship between these systems concerning their superconducting phase diagrams. Both in high-temperature superconductors and in Ga-doped Ge, there is only a limited range of charge-carrier (hole) concentrations which allows for the occurrence of superconductivity, and there is an optimum concentration where the superconducting transition temperature is maximum.

By means of these techniques, we have established a path to fully control the concentration of homogeneously distributed dopants and to activate them as charge carriers. This allows for a clear allocation of the observed superconducting state to the Ga-doped Ge phase, compared to boron-doped diamond where the superconducting state might be attributed to carbon containing boron islands [3].

The preparation techniques for superconducting Ge developed at the FZD can also be used for other dopants and host semiconductors. For this reason, the study of superconducting properties of doped semiconductors can now be performed at a level of quality not previously possible. The exploration of the detailed relation between annealing parameters, carrier density, and critical temperature is under way.

## References

- [1] *Superconductivity in diamond*, E.A. Ekimov, V.A. Sidorov, E.D. Bauer, N.N. Mel'nik, N.J. Curro, J.D. Thompson, S.M. Stishov, Nature 428, 542 (2004)
- [2] *Superconductivity in doped cubic silicon*, E. Bustarret, C. Marcenat, P. Achatz, J. Kacmarik, F. Lévy, A. Huxley, L. Ortéga, E. Bourgeois, X. Blase, D. Débarre, J. Boulmer, Nature 444, 465 (2006)
- [3] *An insight into what superconducts in polycrystalline boron-doped diamonds based on investigations of micro-structure*, N. Dubrovinskaia<sup>1,2</sup>, R. Wirth<sup>3</sup>, J. Wosnitza, T. Papageorgiou, H.F. Braun<sup>2</sup>, N. Miyajima<sup>2</sup>, L. Dubrovinsky<sup>2</sup>, Proceedings of the National Academy of Sciences of the United States of America 105, 11619 (2008); *Large carbon-isotope shift of  $T_c$  in boron-doped diamond*, N. Dubrovinskaia<sup>1,2</sup>, L. Dubrovinsky<sup>2</sup>, T. Papageorgiou, A. Bosak<sup>4</sup>, M. Krisch<sup>4</sup>, H.F. Braun<sup>2</sup>, J. Wosnitza, Applied Physics Letters 92, 132506 (2008)
- [4] *Absence of superconductivity in boron-implanted diamond*, V. Heera, R. Höhne, O. Ignatchik, H. Reuther, P. Esquinazi<sup>5</sup>, Diamond and Related Materials 17, 383 (2008)
- [5] *Superconductivity in Germanium*, T. Herrmannsdörfer, V. Heera, O. Ignatchik, M. Uhlarz, A. Mücklich, M. Posselt, H. Reuther, B. Schmidt, K.-H. Heinig, W. Skorupa, M. Voelskow, C. Wündisch, R. Skrotzki, M. Helm, J. Wosnitza, submitted

## Project partners

- Mineralphysik und Strukturforschung, Mineralogisches Institut, Universität Heidelberg, Germany<sup>1</sup>
- Lehrstuhl für Kristallographie, Bayerisches Geoinstitut, and Physikalisches Institut, Universität Bayreuth, Germany<sup>2</sup>
- GeoForschungsZentrum, Experimental Geochemistry and Mineral Physics, Potsdam, Germany<sup>3</sup>
- European Synchrotron Radiation Facility, Grenoble Cedex, France<sup>4</sup>
- Universität Leipzig, Germany<sup>5</sup>

# New antennas for bridging the terahertz gap

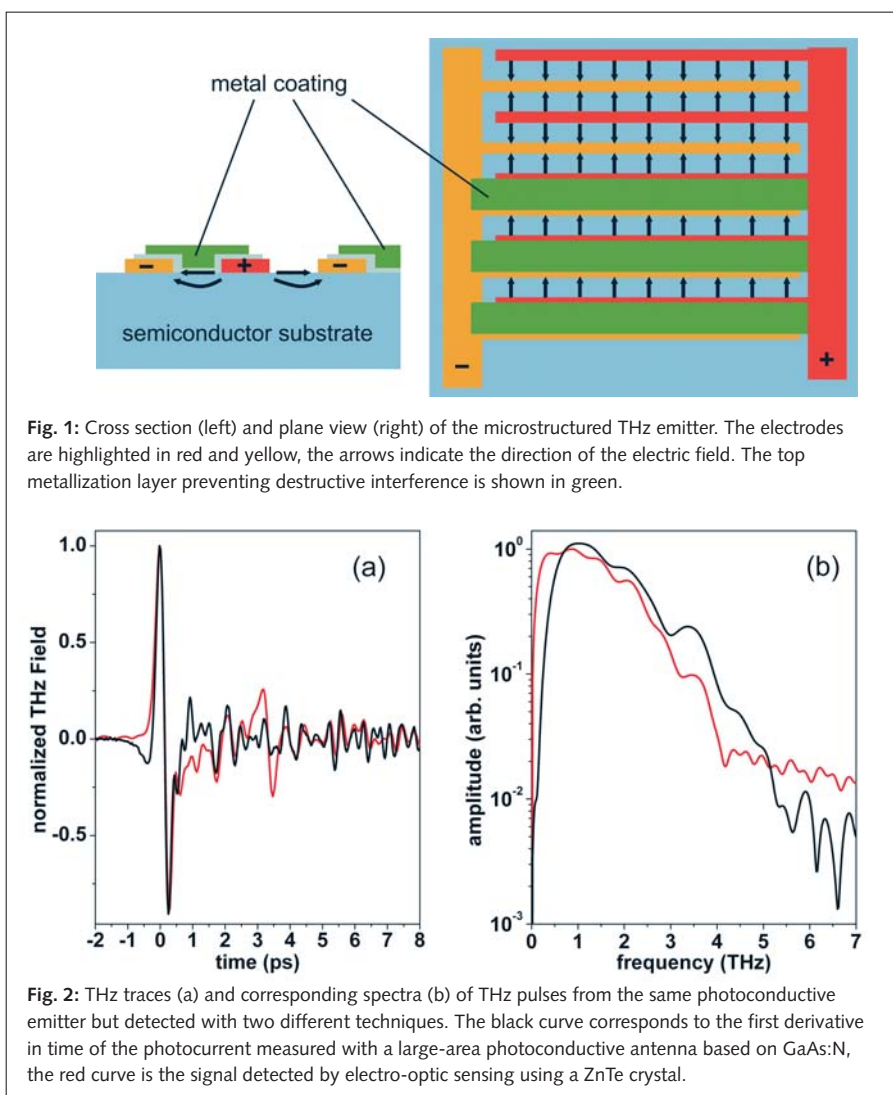
Stephan Winnerl

Terahertz (THz) radiation is electromagnetic radiation in the range from 0.1 to 10 THz (wavelength: 3 mm – 30  $\mu\text{m}$ ). It is the range between microwaves on the low-frequency side and infrared radiation on the high-frequency side. For research, this spectral region is of particular interest, since many elementary and collective excitations, such as phonons and plasmons in solids, inter- and intra-subband transitions in semiconductor quantum structures, as well as vibrations and rotations of molecules, are to be found here. Recently, applications in medical diagnostics, communication technology, process monitoring, and security systems have been explored. For the latter two applications, the transparency of a large number of packaging materials in the THz range is essential. Another important aspect for many possible applications is the non-ionizing nature of THz radiation. However, so far none of the possible applications has reached a larger market. This is owed to the fact that technology in the THz range is still not as mature as in the other regions of the electromagnetic spectrum, which is referred to as the THz gap. Most importantly, there is a lack of powerful, easy-to-use, compact, and reasonably cheap THz sources.

THz-time-domain spectroscopy is a technique able to detect temporally short and spectrally broad THz pulses coherently. It allows for determining both the real and imaginary part of the dielectric function of materials without resorting to Kramers-Kronig relations. Photoconductive antennas excited with ultrashort near-infrared laser pulses are a widely used source of broadband THz radiation. The operation of the antennas is based on the emission of a single-cycle THz wave by photoexcited carriers which are accelerated in an electric bias field. At the FZD, we

have developed a photoconductive emitter with an interdigitated electrode geometry. As can be seen in Fig. 1, the electric field points in opposite directions in neighboring gaps between the electrodes. Destructive interference of THz wavelets from neighboring gaps in the far field is avoided by a second metallization layer preventing optical excitation of every second gap. This concept for scalable large-area emitters combines the advantages, but avoids the drawbacks of two existing concepts of photoconductive antennas, namely

antennas with a small gap allowing large acceleration fields at low bias voltages, on the one hand, and large-area emitters for high-power optical excitation, on the other hand. The patented emitters show higher conversion efficiency from near-infrared to THz power and higher output power compared to conventional antennas [1]. So far, about 60 emitters produced at the FZD have been sold to research groups around the world via GigaOptics GmbH. While other groups have taken up the basic idea of the scalable emitter and performed



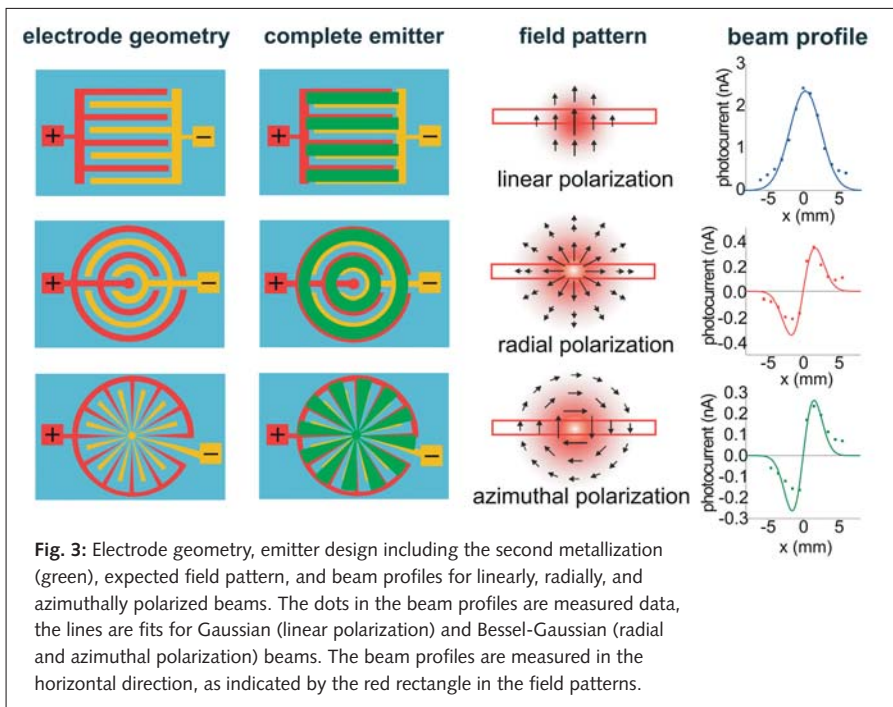


**Fig. 3:** Electrode geometry, emitter design including the second metallization (green), expected field pattern, and beam profiles for linearly, radially, and azimuthally polarized beams. The dots in the beam profiles are measured data, the lines are fits for Gaussian (linear polarization) and Bessel-Gaussian (radial and azimuthal polarization) beams. The beam profiles are measured in the horizontal direction, as indicated by the red rectangle in the field patterns.

column of Fig. 3 and are compared with the calculated lowest-order modes [4]. In the experiment, the beams travelled over a distance of about 0.5 m and were focused on a detector sensitive for linearly polarized radiation (vertical direction for the linear and azimuthally polarized beam, horizontal direction for the radially polarized beam). The radially polarized beams are of great interest due to fundamental properties, such as smaller waists in the focus as compared to Gaussian beams, and strong longitudinal field components in the focus. Apart from that, high coupling efficiencies for radially polarized Bessel-Gauss modes to Sommerfeld modes are expected. Sommerfeld modes are plasmonic guided modes travelling on metal wires. Due to their low attenuation and low dispersion, they are attractive THz waveguides.

research mainly for a different production technology, we have focused on exploring the antennas' potential as a detection unit, adapting the substrate material for excitations with fiber-based lasers, and expanding the idea of the scalable emitter to generate different THz radiation modes.

For detector antennas, the lifetime of photogenerated carriers is an important property. Maximum signal-to-noise ratios can be expected, when the carrier lifetime is comparable to the duration of the THz pulse, i.e. about 1 ps. Low-temperature grown GaAs and GaAs modified by ion implantation are suitable materials. Large-area detection antennas were fabricated with the same electrode geometry as for the emitter discussed above. In Fig. 2, the signal detected with a large-area antenna based on nitrogen-implanted GaAs is compared with the signal obtained by standard electro-optical THz detection using a ZnTe crystal. The main advantage of the large-area detection antenna is that it does not require tight focusing, neither of the THz beam nor the near-infrared gating beam. Therefore, it is easy to align and insensitive against beam-pointing fluctuations [2].

The high price and the complexity of commonly used titanium-sapphire lasers

prevent a more widespread use of pulsed THz systems. In recent years, compact Er-doped fiber lasers and amplifiers operating at a wavelength of 1.55  $\mu\text{m}$  have made great progress. THz emitters excited with fiber lasers require low band gap materials with high resistivity. Microstructured large-area emitters based on InGaAsN grown lattice matched on GaAs were operated successfully for excitation wavelengths up to 1.35  $\mu\text{m}$  [3]. While further optimization of the material – carried out in cooperation with the National Research Council, Ottawa, Canada – is necessary for emitters excited with 1.55  $\mu\text{m}$  radiation, the present InGaAsN emitters are attractive devices for excitation with fiber lasers operated at 1.1  $\mu\text{m}$ .

Finally, the scalable concept is not limited to antennas for generation of linearly polarized light. In principle, any desired THz mode can be generated with an emitter antenna with an electrode geometry inverse to the desired field pattern. In Fig. 3, emitters for linearly, radially, and azimuthally polarized radiation are shown. Radially and azimuthally polarized beams have a donut-like intensity distribution and are the lowest-order modes of the class of Bessel-Gauss beams. Beam profiles measured in the horizontal direction are shown in the last

## References

- [1] *High intensity terahertz radiation from a microstructured large-area photoconductor*, A. Dreyhaupt, S. Winnerl, T. Dekorsy, M. Helm, Applied Physics Letters 86, 121114 (2005); *Kohärente Terahertz-Strahlungsquelle*, T. Dekorsy, M. Helm, A. Dreyhaupt, S. Winnerl, European Patent 1 825 530 B1, granted Oct. 22, 2008
- [2] *Coherent terahertz detection with a large-area photoconductive antenna*, F. Peter, S. Winnerl, S. Nitsche, A. Dreyhaupt, H. Schneider, M. Helm, Applied Physics Letters 91, 081109 (2007)
- [3] *Terahertz emission from a large-area GaInAsN emitter*, F. Peter, S. Winnerl, H. Schneider, M. Helm, K. Köhler<sup>1</sup>, Applied Physics Letters 93, 101102 (2008)
- [4] *Terahertz Bessel-Gauss beams of radial and azimuthal polarization from microstructured photoconductive antennas*, S. Winnerl, B. Zimmermann, F. Peter, H. Schneider, M. Helm, Optics Express 17, 1571 (2009)

## Project partners

- Fraunhofer-Institut für angewandte Festkörperphysik, Freiburg, Germany<sup>1</sup>
- National Research Council, Ottawa, Canada
- GigaOptics GmbH, Konstanz, Germany
- Max-Planck-Institut für Biophysik and Center for Nanoscience, München, Germany
- Fraunhofer-Institut für angewandte Optik und Feinmechanik, Jena, Germany

# Magnetic zinc oxide

Kay Potzger

It is now generally agreed that continuous miniaturization of electronic devices and integrated circuits will come to an end within the next decade. Therefore, new and more powerful mechanisms for future information processing have to be developed. Scientists envision making use of the spin as well – the intrinsic magnetic moment of the electron – in addition to its charge, in the future. Yet, there are still plenty of challenges to overcome for practical so-called spintronic (as opposed to electronic) devices. While an electron cannot lose its particular charge, the spin of the electron can flip when it is scattered on its way through the electric conductor. This phenomenon is called spin decoherence and results in loss of information.

Besides semiconductors – the materials transistors are made of – with large spin coherence, we need materials which can

inject a current of spin-polarized electrons, having all spins pointing in the same direction. One possibility is to connect a ferromagnetic material like iron to the semiconductor. However, the large mismatch between the number of free electrons and their mobility in the metal and in the semiconductor leads to significant decoherence at the interface. Thus, we are working on semiconductors which are ferromagnetic and may serve as such “spin injectors”.

Ferromagnetic semiconductors have been known for half a century. For example, europium oxide possesses mobile electrons which are spin-polarized, since they move through a ferromagnetic crystal. This material, however, is only ferromagnetic at temperatures below 70 K and, thus, not useful for applications. Alternatively, one may dope a common semiconductor with magnetic ions such as iron, cobalt, or nickel. After doping by ion implantation,

the magnetic ions are either built into the regular crystal lattice of the semiconductor or form small embedded magnetic clusters. A highly promising candidate for spin injection is zinc oxide (ZnO) containing magnetic ions.

## Magnetic doping by ion implantation

Ferromagnetic ZnO was created using the ion-beam facility at the FZD. Required large ion fluences and, thus, atomic concentrations are available here. We implanted Fe, Co, and Ni ions at atomic concentrations ranging from 0.5 up to 25 % into the near-surface region of commercial ZnO(0001) single crystals. Besides its potential as ferromagnetic semiconductor, ZnO has a strong self-annealing power. This means that damage created by the accelerated ions hitting ZnO is immediately cured to a certain degree with the possible formation of new material phases. We observed that implantation at different temperatures, i.e. at 623 and 253 K, has a tremendous effect on the magnetic properties.

## Cluster formation at 623 K

After implantation with Fe (Co, or Ni) at 623 K, we observed the formation of magnetic clusters. Only high-resolution analysis techniques, such as synchrotron radiation X-ray diffraction performed at the Rossendorf Beamline in Grenoble, allowed us to identify tiny metallic clusters of Fe, Co, or Ni as the source of ferromagnetism. These clusters exhibit their own distinct crystalline structure. By element-specific measurements it was found that the metallic clusters coexist with dispersed transition-metal ions. The latter are not ferromagnetic. The measurements were performed at the FZD and the Advanced Light Source (ALS) in Berkeley, USA. The unwanted metallic clusters can be avoided by lowering the crystalline

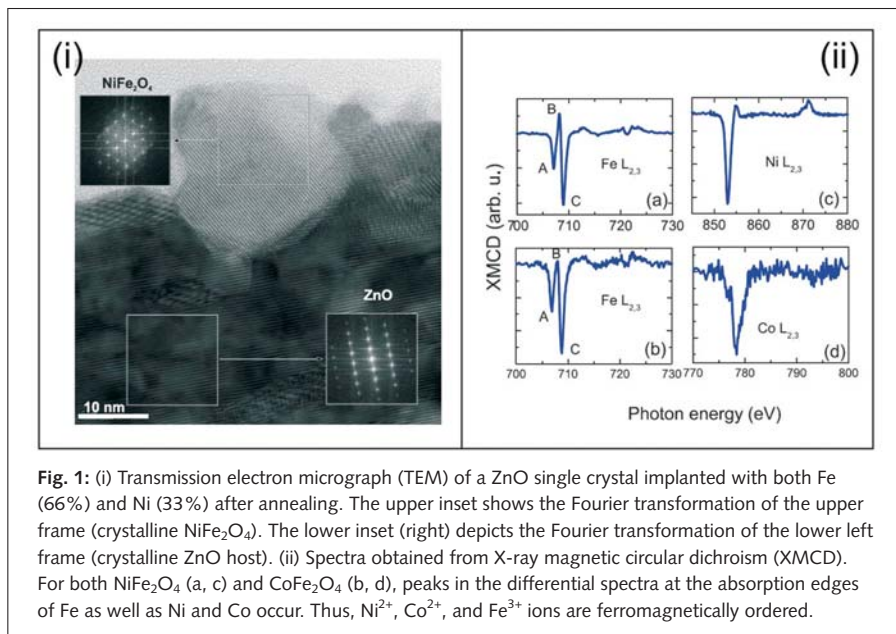


**Fig. 1:** (i) Transmission electron micrograph (TEM) of a ZnO single crystal implanted with both Fe (66%) and Ni (33%) after annealing. The upper inset shows the Fourier transformation of the upper frame (crystalline NiFe<sub>2</sub>O<sub>4</sub>). The lower inset (right) depicts the Fourier transformation of the lower left frame (crystalline ZnO host). (ii) Spectra obtained from X-ray magnetic circular dichroism (XMCD). For both NiFe<sub>2</sub>O<sub>4</sub> (a, c) and CoFe<sub>2</sub>O<sub>4</sub> (b, d), peaks in the differential spectra at the absorption edges of Fe as well as Ni and Co occur. Thus, Ni<sup>2+</sup>, Co<sup>2+</sup>, and Fe<sup>3+</sup> ions are ferromagnetically ordered.



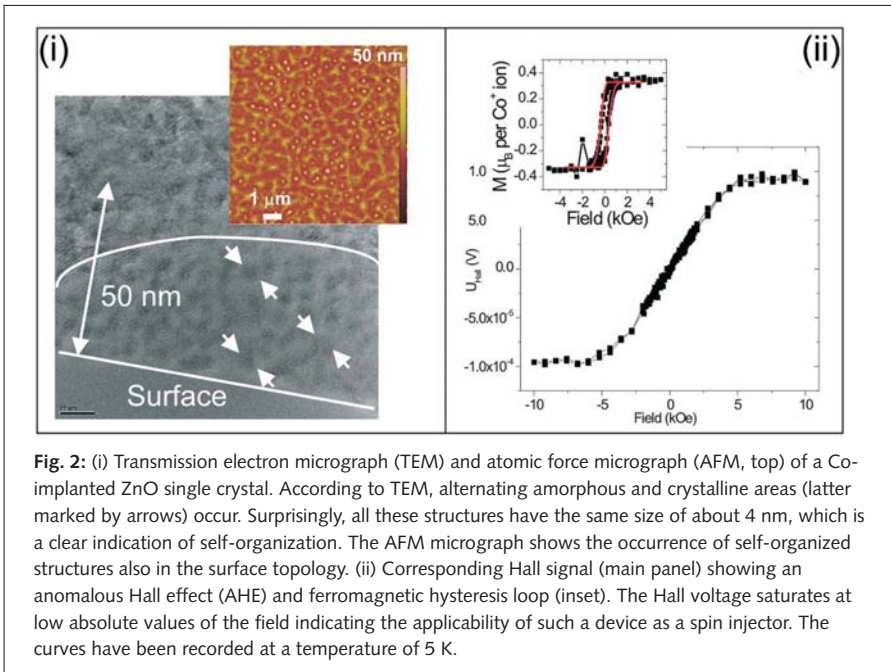


**Fig. 2:** (i) Transmission electron micrograph (TEM) and atomic force micrograph (AFM, top) of a Co-implanted ZnO single crystal. According to TEM, alternating amorphous and crystalline areas (latter marked by arrows) occur. Surprisingly, all these structures have the same size of about 4 nm, which is a clear indication of self-organization. The AFM micrograph shows the occurrence of self-organized structures also in the surface topology. (ii) Corresponding Hall signal (main panel) showing an anomalous Hall effect (AHE) and ferromagnetic hysteresis loop (inset). The Hall voltage saturates at low absolute values of the field indicating the applicability of such a device as a spin injector. The curves have been recorded at a temperature of 5 K.

quality prior to implantation [1]. Then, non-magnetic oxide complexes rather than metallic clusters are formed.

Upon annealing at 823 K, the metallic clusters initially grow due to diffusion. This means that dispersed Co ions stick to already existing clusters, increasing their size. At higher annealing temperatures, the magnetic ions react with Zn and O, forming another kind of material, namely a spinel. Remarkably, the usually anti-ferromagnetic zinc ferrite ( $ZnFe_2O_4$ ) possesses ferromagnetic order due to iron ions having exchanged their positions with zinc ions. For a ferromagnet, one part of the spins of the implanted ions points in one direction and the spins of the other part in the opposite one. In contrast to an antiferromagnet, both parts include different amounts of ions, and, thus, a net ferromagnetic moment occurs. We found that by co-implantation of Fe and Co (or Ni) the spinels Co(or Ni) $Fe_2O_4$  can be

formed which are embedded in ZnO but do not involve zinc (Fig. 1). As well-defined multilayers which are commonly used in microelectronics, such a hybrid nano-material is a promising candidate for spin filtering.

### Cluster formation at 253 K – magnetism in defective/disordered regions

Implantation of Fe, Co, or Ni at low temperatures does not lead to the formation of metallic clusters. Instead, owing to the ZnO damages from the ion bombardment, exotic magnetic phases are created. Two of them are presented here. In the first case, clusters of agglomerated defects lead to weak ferromagnetism. We assume that electrons in such defects occur in a triplet state, where their spins do not compensate each other. Such situations can also be found in oxygen molecules where two electrons from the chemical bond have parallel spins. Our defect clusters in ZnO show only a weak

dependence of the magnetization on temperature. Such defect-induced ferromagnetism can also occur if ZnO is grown as thin films on a substrate. By adjusting such growth parameters as temperature and partial pressure of nitrogen gas in the growth chamber, defect-induced ferromagnetism can be obtained [2].

In the second case, Co-doped ZnO becomes ferromagnetic due to structural disorder induced by the bombardment with large Co-ion fluences (Fig. 2). The disordered regions exhibit locally large Co and low O concentrations leading to a metallic-like behavior of the Co and, thus, ferromagnetism originating from direct overlap of the 3d electrons [3].

### References

- [1] *Suppression of secondary phase formation in Fe implanted ZnO single crystals*, K. Potzger, Shengqiang Zhou, H. Reuther, K. Kuepper, G. Talut, M. Helm, J. Fassbender, J.D. Denlinger, Applied Physics Letters 91, 062107 (2007)
- [2] *Room temperature ferromagnetism in ZnO films due to defects*, Qingyu Xu, H. Schmidt, Shengqiang Zhou, K. Potzger, M. Helm, H. Hochmuth, M. Lorenz, A. Setzer, P. Esquinazi, C. Meinelcke, M. Grundmann, Applied Physics Letters 92, 082508 (2008)
- [3] *Ferromagnetic, structurally disordered ZnO implanted with Co ions*, K. Potzger, Shengqiang Zhou, Qingyu Xu, A. Shalimov, R. Groetzschel, H. Schmidt, A. Mücklich, M. Helm, J. Fassbender, Applied Physics Letters 93, 232504 (2008)

### Project partners

- Universität Leipzig, Germany
- Advanced Light Source, Berkeley, USA
- European Synchrotron Radiation Facility, Grenoble, France

# Self-organized surface nanopatterns induced by low-energy ion erosion

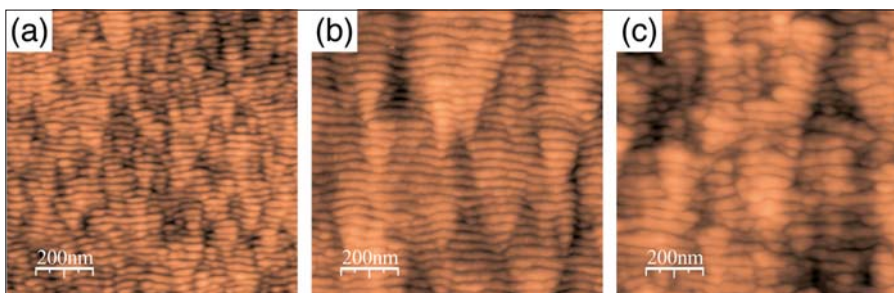


**Fig. 1:** Atomic force microscopy images of Si surfaces after sputtering with 500 eV  $\text{Ar}^+$  ions at  $67^\circ$  incidence (with respect to the surface normal). The applied ion fluences are  $1 \times 10^{17}$  (a),  $1.7 \times 10^{18}$  (b), and  $1 \times 10^{19}$  ions per  $\text{cm}^2$ .

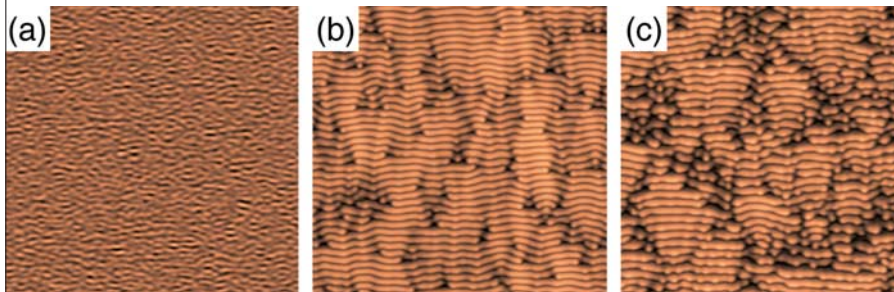


**Fig. 2:** Surface morphologies resulting from numerical integrations of the damped Kuramoto-Sivashinsky equation for the parameters and fluences corresponding to those given in Fig. 1.

Stefan Facsko, Adrian Keller

The need for sub-micron scale functional structures in today's micro- and optoelectronics has motivated an increase in such research over the past few years. There are two complementary approaches to produce such nanometer sized features: the *top-down* and the *bottom-up* approach. The first case is represented by conventional processes like electron-beam lithography whereas in the latter case self-organization phenomena are used. A promising bottom-up technique for the large-scale fabrication of periodic nano-

structure arrays is the self-organized formation of nanoscale ripple patterns during oblique ion bombardment of solid surfaces. The impinging ions penetrate the surface, losing their kinetic energy and momentum in collisions with surface atoms. These collisions can lead to a removal of surface material; the mechanism is called *sputtering*. During the sputter process, the morphology of the surface changes and, under certain conditions, regular nanopatterns evolve. These patterns have been found in a large variety of materials including insulators, semiconductors, and metals. Their

periodicity is determined by the experimental conditions and ranges from roughly 15 nm up to more than 1  $\mu\text{m}$ .

## Evolution of ion-induced ripple patterns

We are studying the formation and evolution of nanoscale ripple patterns during sub-keV ion sputtering with the aim to precisely control the pattern properties for certain applications. Fig. 1 shows three stages of the evolution of Si surfaces during sputtering with 500 eV  $\text{Ar}^+$  ions at  $67^\circ$  incidence [1, 2]. At low fluences (number of incoming ions per surface area), a pattern of shallow ripples is obtained (Fig. 1a). At an intermediate stage (Fig. 1b), larger corrugations overlay the ripple pattern and get more pronounced. At high fluences (Fig. 1c), the surface enters a steady state with a more disordered ripple pattern. A quantitative analysis of the pattern quality reveals a rather sharp optimum at intermediate fluences [2]. In addition, the ripple wavelength is observed to increase from initially  $\sim 24$  nm (Fig. 1a) to  $\sim 40$  nm (Fig. 1c) [1]. This nonlinear phenomenon is called *ripple coarsening*. Coarsening is observed only in some experimental systems and up to now far from being understood.

## Theoretical modeling

The formation and long-time evolution of the ion-induced ripple patterns can be modeled by nonlinear partial differential equations, which consider the surface as a continuous height function. Several of these nonlinear continuum models have been proposed. We are performing numerical integrations of some of these models in order to reproduce our

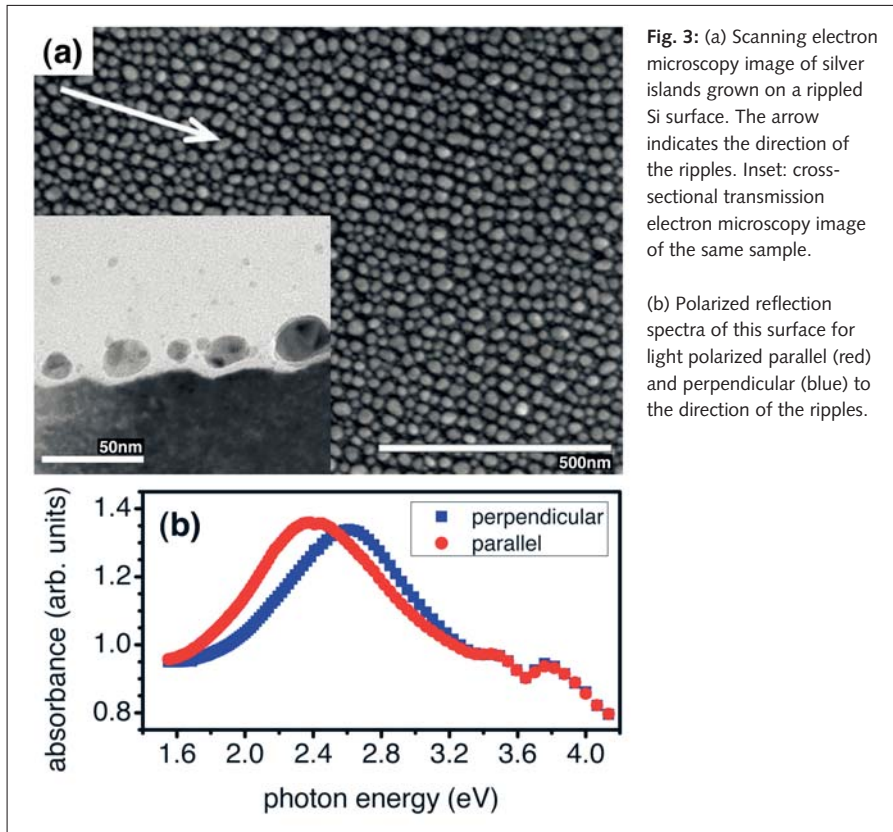


**Fig. 3:** (a) Scanning electron microscopy image of silver islands grown on a rippled Si surface. The arrow indicates the direction of the ripples. Inset: cross-sectional transmission electron microscopy image of the same sample.

(b) Polarized reflection spectra of this surface for light polarized parallel (red) and perpendicular (blue) to the direction of the ripples.

known to exhibit a so-called *plasmon resonance*, i.e. the absorption of incident light of well-defined energy by oscillating electrons in the islands. In the case of nanoparticle chains produced on rippled substrates, however, this plasmon resonance is found to depend on the polarization, i.e. the direction of its electric field vector, of the incident light [3]. This can be seen in the reflection spectra shown in Fig. 3b, where the absorption maximum is red-shifted for light polarized parallel to the direction of the ripples. This effect can be understood by a collective excitation of the oscillating electrons in nearby islands which are closer to each other along the valley. With the same technique arrays of continuous metal nanowires can also be produced [4]. Such metallic nanostructure arrays are of great interest for certain applications, e.g. in chemical sensing and catalysis, or as dichroic filters.

experimental observations. Fig. 2 shows a simulation of the so-called damped Kuramoto-Sivashinsky equation at three stages, corresponding to the experimental surfaces given in Fig. 1. The simulations show good qualitative agreement with the experiments and are even able to quantitatively reproduce the evolution of the pattern quality [2]. However, the observed ripple coarsening cannot be reproduced by the simulations. This demonstrates that more experimental and theoretical work is needed in order to understand the basic mechanisms of ion-induced pattern formation. Therefore, we are performing further experiments on different surfaces in order to investigate

the dependence of ripple coarsening on various experimental parameters, like ion energy or incident angle.

#### Application in thin-film growth

Rippled surfaces have been used successfully as pre-patterned templates in thin film growth. In this way, we are able to modify certain physical film properties in a controlled fashion. Fig. 3a shows an array of silver islands which have been grown on rippled Si surfaces by physical vapor deposition. The islands are aligned along the ripples, forming chains. The cross-sectional view in the inset of Fig. 3a shows that the islands preferentially sit in the ripple valleys. Such silver islands are

#### References

- [1] *Simultaneous formation of two ripple modes on ion sputtered silicon*, A. Keller, S. Roßbach, S. Facsko, W. Möller, *Nanotechnology* 19, 135303 (2008)
- [2] *Minimization of topological defects in ion-induced ripple patterns on silicon*, A. Keller, S. Facsko, W. Möller, *New Journal of Physics* 10, 063004 (2008)
- [3] *Aligned silver nanoparticles on rippled silicon templates exhibiting anisotropic plasmon absorption*, T.W.H. Oates<sup>1</sup>, A. Keller, S. Facsko, A. Mücklich, *Plasmonics* 2, 47 (2007)
- [4] *Self-organized metallic nanoparticle and nanowire arrays from ion-sputtered silicon templates*, T.W.H. Oates<sup>1</sup>, A. Keller, S. Noda<sup>1</sup>, S. Facsko, *Applied Physics Letters* 93, 063106 (2008)

#### Project partner

· University of Tokyo, Japan<sup>1</sup>

# Commissioning of the superconducting radiofrequency photoelectron injector at ELBE



**Fig. 1:** SRF photoinjector in the ELBE accelerator hall. Left side: vacuum vessel with the helium transfer line on top. Right side: electron beamline with the emittance compensation solenoid, the laser input port, the first screen station, and three quadrupole magnets.

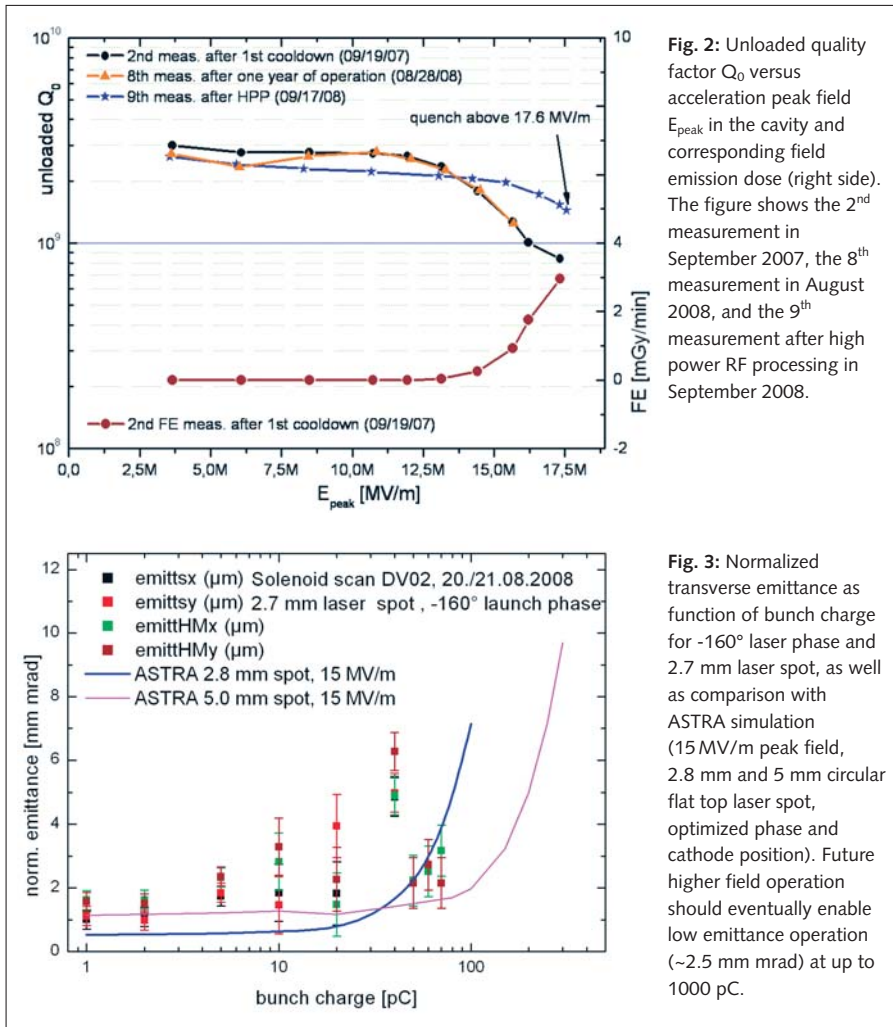
Jochen Teichert

Many of the most exciting and demanding applications for electron accelerators, including future free-electron lasers, energy recovery linacs, and 4th generation light sources, require electron beams with an unprecedented combination of high brightness, low emittance, and high average current. For that reason, existing electron injectors must be considerably improved, or new injector concepts must be developed. One very promising approach is the superconducting radio frequency photoinjector (SRF gun). State-of-the-art conventional photoelectron injectors (using normal conducting RF) can deliver electron beams of the highest brightness, but with low average current only. Superconducting acceleration technology is the most suitable for high

average currents because of the very low RF losses and the straightforward continuous wave operation. The new SRF gun at the ELBE facility combines these two advantages. It will improve the beam quality in several respects, and is a center piece of our future developments in advanced radiation and particle sources: The experiments with neutrons and positrons both require lower pulse repetition rates. With the new injector, this will not reduce the average current since the bunch charge can be increased. For the FEL operation at ELBE a higher stability, higher power of the infrared beam, and an extended parameter range can be expected. Also, better electron beam quality is an essential ingredient for future experiments which will combine the ELBE electron beam with the new ultra high-intensity laser system, "Draco".

Even though proposed about twenty years ago, the SRF gun at ELBE is the first operating injector of this type installed at an accelerator worldwide. The greatest challenges have been the development of a suitable acceleration cavity and the difficulties associated with the photo cathode. In 2002, it was shown in a proof-of-principle experiment at the FZD that a normal-conducting semiconductor photo cathode can be operated in a superconducting cavity, and the first electron beam could be produced with a SRF gun [1]. In 2004, the R&D project for the ELBE SRF gun was launched. The injector together with the UV driver laser system and the diagnostic beamline were developed and constructed within a collaboration of the German institutes BESSY Berlin, DESY Hamburg, MBI Berlin, and the FZD. A major part of the project costs has been financed from external funds of the European Commission within the FP6 Program, and the German Federal Ministry of Education and Research.

The SRF gun cryomodule was installed in July and the first cool-down was performed in August 2007. In the following weeks, the RF system was put into operation and the driver laser system was installed. The autumn shut-down of ELBE was used to complete the installation of the diagnostic beamline. A photograph of the SRF gun after completed installation is shown in Fig. 1. At the end of October 2007, the gun was cooled down for the second time. The first accelerated beam was produced on November 12, 2007 using a copper photo cathode. The remainder of 2007 was spent for commissioning and testing the diagnostic beamline components. In March 2008, the cathode transfer system was completed, and the first Cs<sub>2</sub>Te photo cathodes were inserted



These results are in good agreement with an ASTRA simulation for roughly the same RF gradient (15 MV/m peak field) and laser spot size (2.8 mm diameter). Here, the predicted operation limit is 100 pC, due to the growing space charge effect in front of the photo cathode, for this modest peak electric field value. The simulation also shows that for an optimized laser spot (5 mm) the limit can be shifted towards 200 to 300 pC. The larger laser spot reduces the space charge effect at higher bunch charges, but increases the transverse emittance at low bunch charges due to the thermal emittance which is proportional to the laser spot size.

The gun has been in operation for about 500 hours without serious problems. The electron beam has been produced with a Cu photo cathode, and subsequently with Cs<sub>2</sub>Te photo cathodes. The gun was always operated in continuous wave mode, with an average beam current of about 1  $\mu$ A. As discussed above, a degradation of the cavity, due to pollution from the photo cathode or due to other reasons, was not observed. The lifetime of the photo cathodes was sufficient for our intended use in ELBE.

In the next run in 2009, the gun will be operated with optimized operation parameters at higher acceleration field and 3 MeV electron beam energy. This should allow larger bunch charges of up to 500 pC while maintaining good emittance. We shall continue the gun performance measurements and parameter optimization, operate the gun at high average current, and also produce the first beams for injection into ELBE.

#### Reference

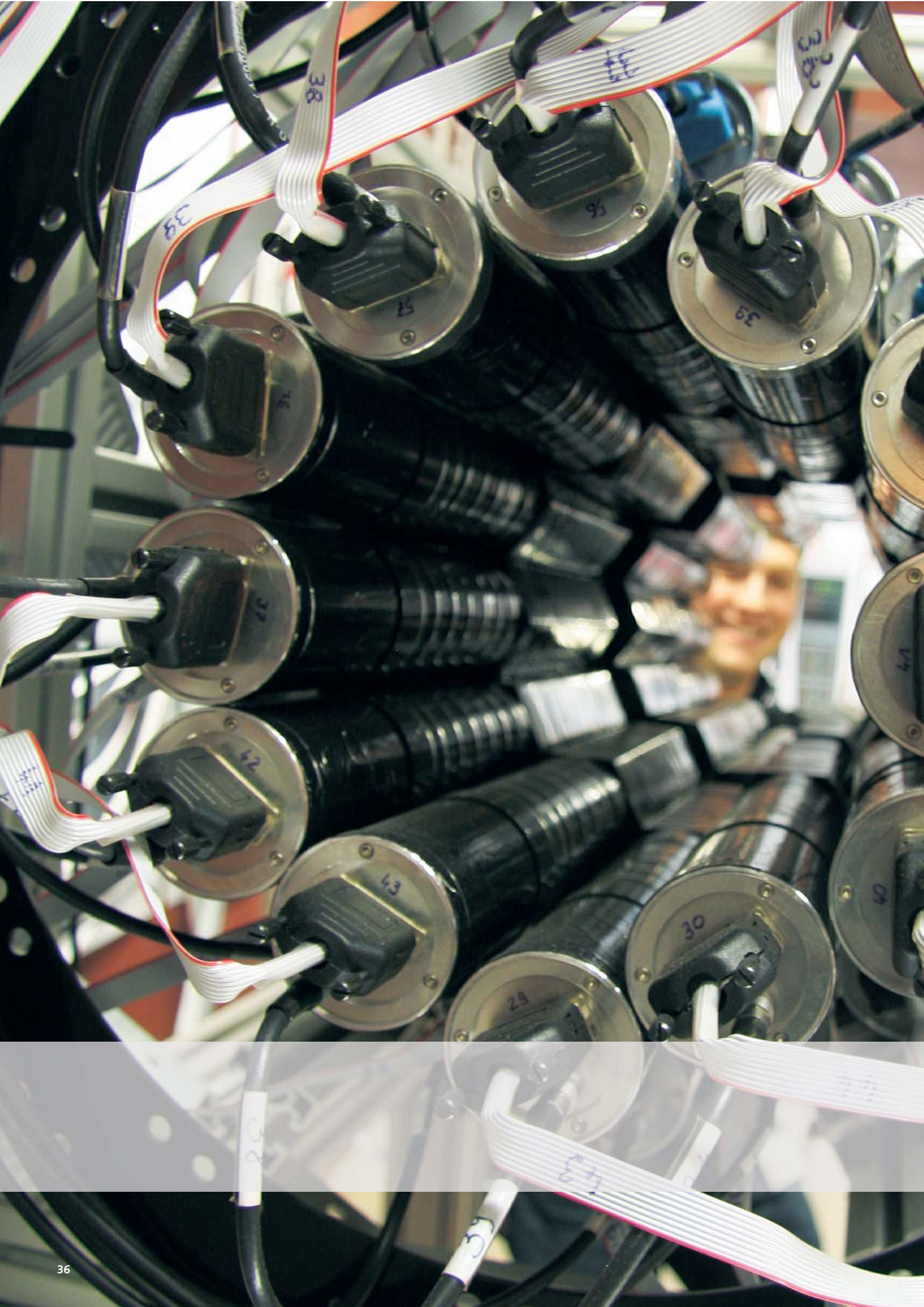
- [1] *Development of a superconducting radio frequency photoelectron injector*, A. Arnold, H. Büttig, D. Janssen, T. Kamps, G. Klemz, W.D. Lehmann, U. Lehnert, D. Lipka, F. Marhauser, P. Michel, K. Möller, P. Murcek, Ch. Schneider, R. Schurig, F. Staufenberg, J. Stephan, J. Teichert, V. Volkov, I. Will, R. Xiang, Nuclear Instruments and Methods in Physics Research A 577(3), 440 – 454 (2007)

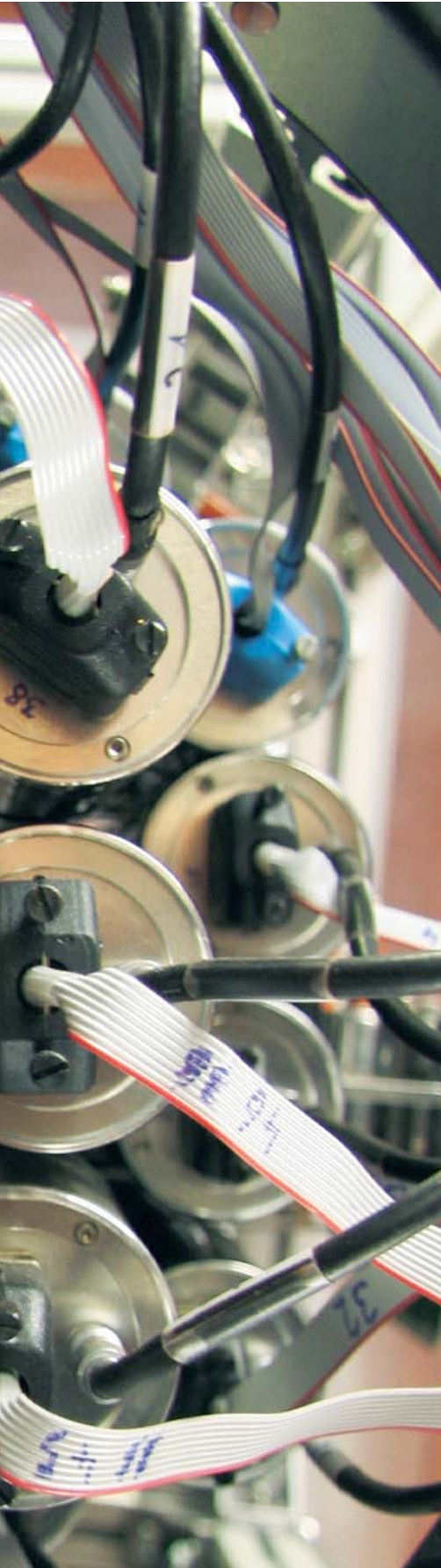
into the gun. From May until September 2008, the gun was operated with these photo cathodes.

A critical aspect of the gun operation is its RF performance. The most important RF measurement is related to the unloaded quality factor  $Q_0$  and the obtained acceleration field  $E_{\text{peak}}$  in the cavity. The results for the  $Q_0$  versus  $E_{\text{peak}}$  curve are presented in Fig. 2. The comparison of the measurements, after installation in 2007, and at the end of the first operational period in August 2008, does not show any performance deterioration of the cavity. The red curve displays the corresponding radiation level caused by field emission in the cavity. As already observed in the former vertical cryostat tests, the reduction in  $Q_0$  is connected to field emission. At the end of the measurement period in

September 2008, a high RF power processing (HPP) of the cavity was carried out. This treatment improved the cavity to a peak field of 17.5 MV/m (6.5 MV/m acceleration gradient) as shown by the blue curve.

During the first tests producing electron beams, the SRF gun was operated with an acceleration gradient of 5 MV/m, and an electron beam energy of 2.05 MeV. This was a conservative choice, at about 20 % of the ultimate design goal. The transverse emittance as a function of bunch charge was measured using the solenoid scan method, and the results are presented in Fig. 3. For lower bunch charge, the measured transverse emittance is between 1 and 2 mm mrad. At about 40 pC, the emittance begins to increase and measurements could be performed up to 80 pC.



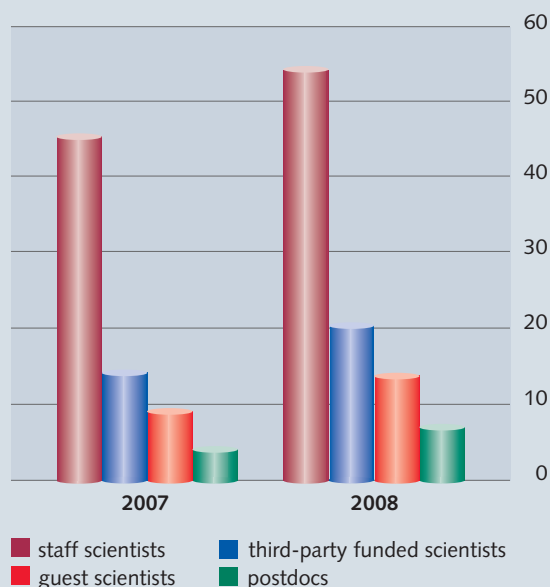


The Forschungszentrum Dresden-Rossendorf (FZD) is a multi-disciplinary research center for natural sciences and technology. It is the largest institute of the Leibniz Association and is equally funded by the Federal Republic of Germany and the Federal States, in particular by the Free State of Saxony. At the FZD, around 330 scientists are engaged in three different research programs of basic and application-oriented research. Scientists working in the Advanced Materials Research program investigate the reactions of matter in strong fields and at small dimensions. Research and development in the Cancer Research program is focused on the imaging of tumors and the effective radiation treatment of cancer. How can humankind and the environment be protected from technical risks? – This question is in the center of research in the Nuclear Safety Research program of the FZD.

In the following Facts & Figures section data presenting the scientific output in the Advanced Materials Research program are given as well as information on staff and funding at the FZD.

## Facts & Figures

### Scientific staff – Advanced materials research

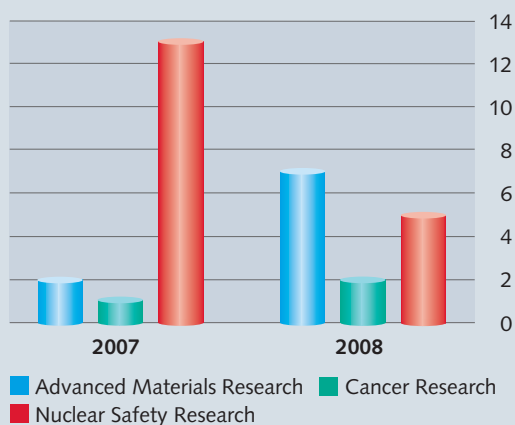


Distribution of positions occupied by scientific personnel in the Advanced Materials Research program of the FZD. Third-party funded scientists, guest scientists, and postdocs represented by the corresponding figures are given in units of paid full-time posts.\*

Budget	2007		2008	
	Core Funding T€	Third-Party Funding T€	Core Funding T€	Third-Party Funding T€
Research Programs				
<b>Advanced Materials Research</b>	<b>19.776</b>	<b>1.600</b>	<b>17.822</b>	<b>4.622</b>
Cancer Research	7.729	1.141	9.340	840
Nuclear Safety Research	12.577	5.086	13.069	3.660
Large-Scale Facilities	14.564	1.487	18.401	4.028
<b>Sum</b>	<b>54.646</b>	<b>9.314</b>	<b>58.632</b>	<b>13.150</b>

Share of each research program, as well as of the experimental facilities located at the FZD, of both core and third-party funding during the last two years.

### Patents – FZD

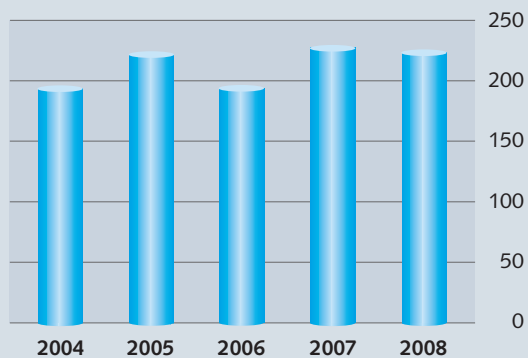


Number of applications for a patent filed in each research program of the FZD in 2007 and 2008.

\*All figures as of 1st March 2009.

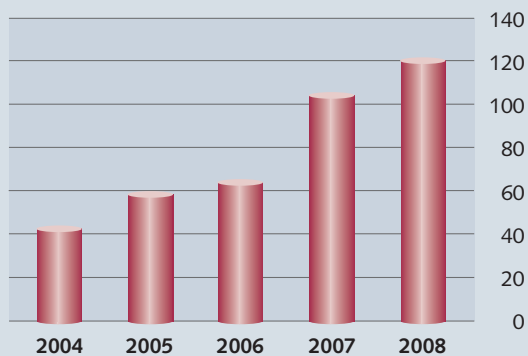


**Publications – Advanced materials research**



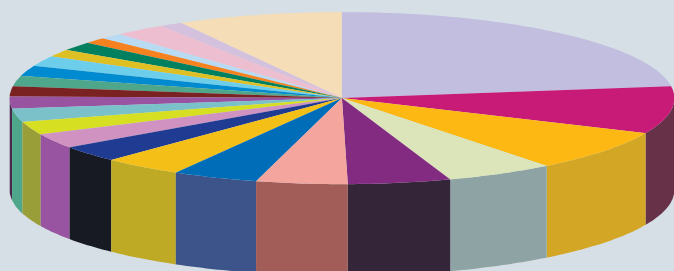
Number of peer-reviewed articles by scientists from the FZD's Advanced Materials Research program.

**Doctoral students – FZD**



Growth in number of doctoral students at the FZD from 2004 until 2008.

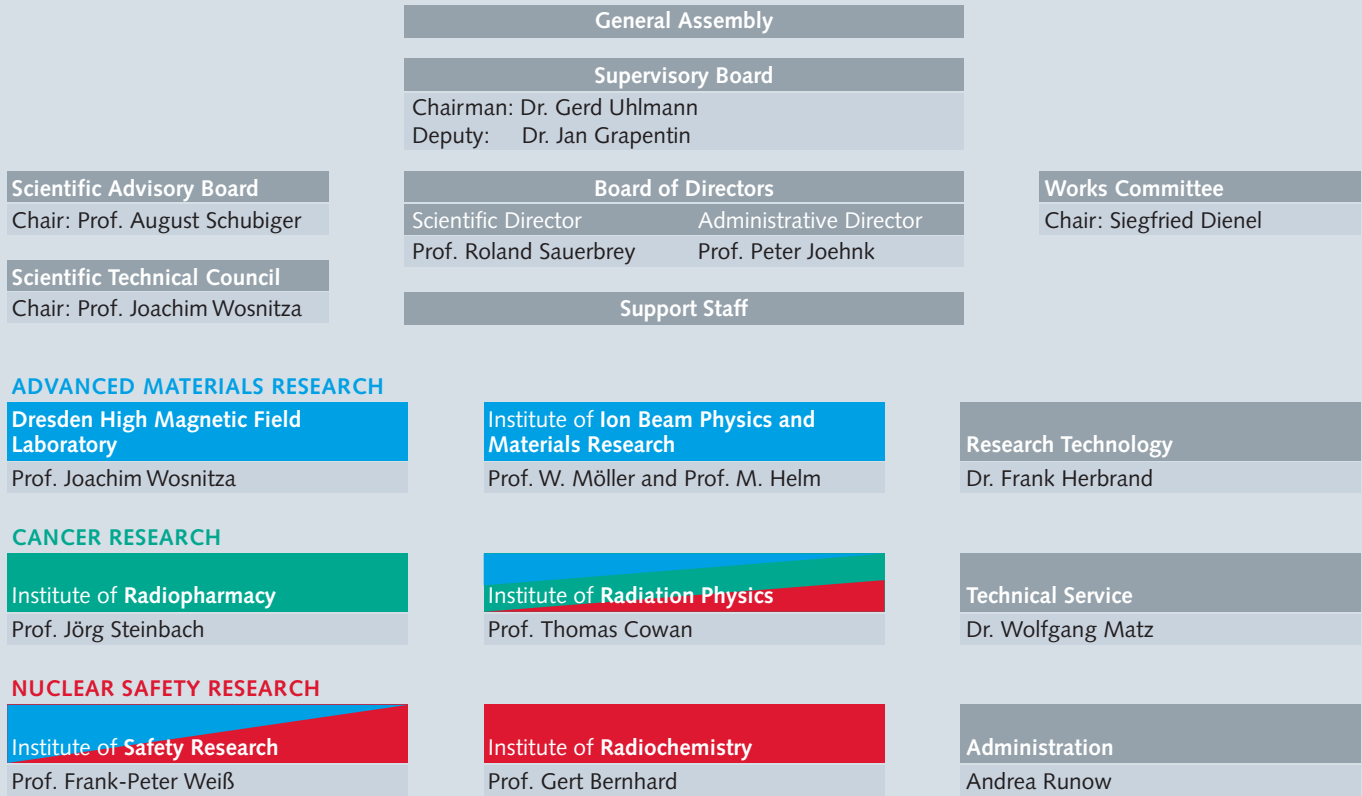
**International guest scientists – FZD**



Distribution of the international guest scientists who visited the FZD for the purpose of research between 2007 and 2008 according to their countries of origin.

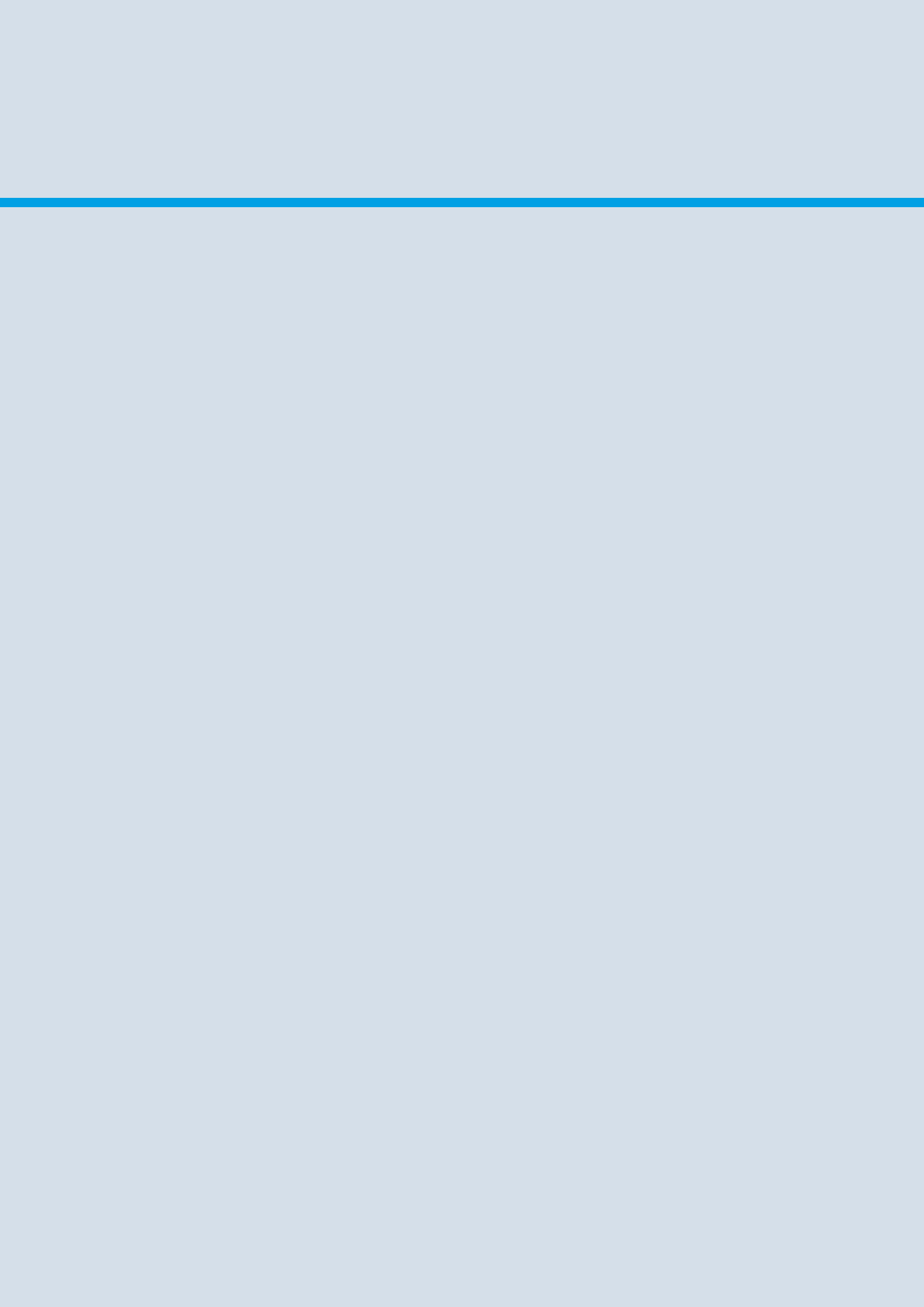
Russia	59	USA	11	Japan	6	Latvia	4
Czech Republic	23	Bulgaria	10	Turkey	6	Portugal	4
Poland	20	China	8	France	5	Algeria	3
Ukraine	14	Australia	7	Netherlands	5	Egypt	3
India	13	Italy	7	Romania	5	Israel	3
Hungary	11	Great Britain	6	Spain	5	others	21

## Organizational Chart



■ Advanced Materials Research
 ■ Cancer Research
 ■ Nuclear Safety Research

March 2009





**Forschungszentrum Dresden - Rossendorf**

P.O. Box 51 01 19 | 01314 Dresden/Germany

Scientific Director | Prof. Dr. Roland Sauerbrey

Phone +49 351 260 2625

Fax +49 351 260 2700

Email [contact@fzd.de](mailto:contact@fzd.de)

[www.fzd.de](http://www.fzd.de)

Member of the Leibniz Association